PHYSICAL REVIEW A

ATOMIC, MOLECULAR, AND OPTICAL PHYSICS

THIRD SERIES, VOLUME 49, NUMBER 5 PART B — MAY 1994

ARTICLES

Quantum field theory of interaction of ultracold atoms with a light wave: Bragg scattering in nonlinear atom optics

Weiping Zhang

School of Mathematics, Physics, Computing and Electronics, Macquarie University, New South Wales 2109, Australia

D. F. Walls

Physics Department, University of Auckland, Auckland, New Zealand

(Received 18 May 1992; revised manuscript received 1 February 1993)

A vector quantum field theory is developed to describe the interaction of an ultracold atomic ensemble with a laser field. The ultracold atomic ensemble is composed of either bosonic atoms or fermionic atoms. The photon exchanges between different ultracold atoms result in a long-range interatom interaction. Under appropriate conditions, such a many-body interaction leads to an effective "Kerr-type" nonlinearity of atomic waves. In terms of the nonlinearity, we construct a general formalism of nonlinear atom optics for an ultracold atomic beam. Applying the formalism to the diffraction of an ultracold atomic beam composed of bosonic atoms by a standing-wave laser field, we find that the many-body nonlinearity induces self-phase and cross-phase modulation of diffracted atomic waves. As a result, a standing-wave laser acts as a nonlinear atomic grating which diffracts atoms in the same way as a nonlinear periodic medium diffracts photons.

PACS number(s): 03.75.Be, 42.50.Vk, 32.80.Pj

I. INTRODUCTION

In the past few years, rapid progress was made in laser cooling and trapping of neutral atoms [1–6]. By cooling techniques of neutral atoms, one can reduce thermal motion of an atom and achieve a long thermal de Broglie wavelength. Such cold atoms provide necessary tools to study optical effects of atoms in atom optics [7].

On the other hand, the combination of optical cooling and atom traps introduces the possibility of producing ultracold atomic sources where bosonic atoms are expected to lose their individual identities and degenerately condense into a macroscopic single quantum state at extremely low temperatures together with sufficiently high densities. Such atomic sources are expected to have properties similar to the role of lasers in conventional coherent optics.

Although there are many limitations to the generation of an ultracold quantum state of atoms in an optical trap [8,9], in principle it is possible to realize such a quantum state by other cooling and trapping techniques, for example, evaporative cooling, magnetic traps, and atomic cavities [10–13]. By combination of different cooling and trapping techniques, the temperatures and densities achieved in current experiments are $T \sim 1\ \mu\text{K}$, $n \sim 10^{10}$ cm^{-3} for cesium atoms [5] and $T \sim 100\ \mu\text{K}$, $n \sim 8\times 10^{13}$ cm^{-3} for hydrogen atoms [6]. Such temperatures and densities bring the samples towards the critical points of Bose-Einstein condensation and the effect of quantum statistics on the behavior of the samples in the near-critical conditions should be of crucial importance. Particularly, quantum statistics lead to new aspects in atom optics if the atomic beams used in current experiments of atom optics are replaced by those from ultracold atomic sources.

The existing theory for interaction of atoms with light waves adopted either a single-particle density-operator equation or a Schrödinger equation to describe the center of mass motion of atoms, which forms the theoretical basis for laser cooling and atom optics [14–22]. Such a single-particle description is valid since the current experiments in these areas only involve low-density atomic samples. However, for ultracold atomic samples, the single-particle theory is no longer valid and many-body quantum statistics must be taken into account. In this paper, we develop a quantum statistical theory for interaction of ultracold atoms with light waves in the framework of a vector quantum field theory. As a general description, the ultracold atomic sample is assumed to be composed of either bosonic atoms or fermionic atoms. Considering a typical example in atom optics, we apply the theory to the diffraction of an ultracold atomic beam by a standing-wave laser. For simplicity, the Bragg resonance condition [16] is assumed in the diffraction of ultracold atoms. In this case, we find that the standing-wave laser acts as a nonlinear atomic beam splitter in the ultracold regime. By employing this simple example, we present our basic ideas in constructing a formalism of nonlinear atom optics for an ultracold atomic beam in the framework of quantum field theory.

This paper is a detailed extension of our previous papers [23–26] and is organized as follows: Sec. II describes the quantum field theory of interaction of ultracold atoms with a laser field. A general vector nonlinear stochastic Schrödinger equation for ultracold atoms and a general quantum propagation equation for laser photons are obtained which form the basis to study atomic nonlinear phenomena in atom optics and quantum optics. Applying the nonlinear stochastic Schrödinger equation of ultracold atoms and the quantum propagation equation of laser photons, we develop a general formalism of nonlinear atom optics for an ultracold atomic beam in Sec. III. Two sources of the atomic nonlinearity are identified by considering a standing-wave laser. In Sec. IV we study the effects of atomic nonlinearity induced by the absorption and dispersion of laser photons on the diffraction of atoms. The results show that the absorption of photons tends to reduce the intensity of the standing-wave laser and the dispersion of photons does distort the periodic structure of the standing-wave laser. As a result, the standing-wave laser is no longer a perfect diffraction grating for an ultracold atomic beam when the absorption and dispersion of photons is not negligible. The conditions necessary to eliminate the effects of absorption and dispersion of laser photons are discussed. In Sec. V we study the nonlinear diffraction of ultracold atoms by a standing-wave laser with a negligible absorption and dispersion. The Bragg resonance condition is employed to simplify our discussions for the diffraction. In this case, the standing-wave laser acts as a nonlinear splitter of an ultracold atomic beam. By analogy with the propagation of a light wave in an optical Kerr-type nonlinear medium, we find that the long-range interatomic interaction due to photon exchanges leads to an atomic "Kerr-type" nonlinearity which induces self-phase modulation (SPM) and cross-phase modulation (XPM) of diffracted atomic waves. Such nonlinear phase modulations result in a diffraction dynamics of an ultracold atomic beam which is fully different from that of a single-atom beam. A numerical simulation for nonlinear Bragg scattering of an ultracold atomic beam is given in Sec. VI. The conclusions are included in Sec. VII.

II. QUANTUM FIELD THEORETIC DESCRIPTION OF ULTRACOLD ATOMS

The interaction theory of a single atom with a laser beam including the center of mass motion of atoms has well been developed [14–22]. In the single-atom theory, the dynamic behavior of atoms is described by either a single-particle density operator equation or a Schrödinger equation. In this section, we develop a many-body quantum statistical theory for ultracold atomic ensembles using quantum field theory. In order to take quantum statistics into account, we describe the ultracold atomic ensembles as a vector quantum field with different internal levels instead of the description of the conventional single-particle wave function. In terms of our previous papers [23–26] and Ref. [27], in the dipole approximation the single-particle Hamiltonian for a moving two-level atom interacting with a quantized laser field has the form

$$
\begin{aligned}
&H = H_A + H_L + H_F + H_{A\text{-}L} + H_{A\text{-}F} ,\\
&H_A = -\frac{\hbar^2\nabla^2}{2m} + \hbar\omega_a \sigma^\dagger \sigma ,\\
&H_L = \frac{1}{2}\int d^3r \left[\varepsilon_0 \left[\frac{\partial \mathbf{A}}{\partial t} \right]^2 + \frac{1}{\mu_0}(\nabla\times\mathbf{A})^2 \right] ,\\
&H_F = \sum_{\mathbf{k}\lambda} \hbar\omega_{\mathbf{k}} B^\dagger_{\mathbf{k}\lambda} B_{\mathbf{k}\lambda} ,\\
&H_{A\text{-}L} = -\mathbf{J}\cdot\mathbf{A} = -(\mathbf{J}_{12}\sigma + \mathbf{J}_{21}\sigma^\dagger)\cdot\mathbf{A} ,\\
&H_{A\text{-}F} = -\hbar\sum_{\mathbf{k}\lambda} g^*_{\mathbf{k}\lambda} B^\dagger_{\mathbf{k}\lambda} \exp(-i\mathbf{k}\cdot\mathbf{r})(\sigma+\sigma^\dagger) + \text{H.c.} ,
\end{aligned}
\tag{1}
$$

where H_A, H_L, and H_F are, respectively, the free Hamiltonian of the moving atom with resonance frequency ω_a, of the quantized laser field with frequency ω_L, and of the vacuum electromagnetic field which is introduced to describe the effect of the spontaneous emission of the atoms. The Hamiltonian $H_{A\text{-}L}$ describe the interaction of the atom with the laser field with vector potential $\mathbf{A}$. $H_{A\text{-}F}$ is the interaction Hamiltonian of the atom with the vacuum electromagnetic field. Vector $\mathbf{J}_{ij} = i\omega_L \boldsymbol{\mu}_{ij}$ $(i \neq j = 1,2)$ is the matrix element of the transverse-electric-current operator $\mathbf{J}$ and $\boldsymbol{\mu}_{ij}$ is the matrix element of dipole moment of the atom [27]. Here we take $\boldsymbol{\mu}_{ij} = \boldsymbol{\mu}_{ji} = \boldsymbol{\mu}$ as a real number. $B^\dagger_{k\lambda}$ and $B_{k\lambda}$ are the bosonic creation and annihilation operators of the vacuum electromagnetic field. The coefficient $g_{\mathbf{k}\lambda} = i(2\pi\omega_k/\hbar V_e)^{1/2}\, \boldsymbol{\mu}\cdot\mathbf{e}_{\mathbf{k}\lambda}$ is the coupling strength of the atom with the vacuum electromagnetic fields. The atomic transition is described by the Pauli spin operators σ and $\sigma^\dagger$.

For an ultracold atomic ensemble which is composed of many bosonic atoms or fermionic atoms, the total Hamiltonian should be the sum over all atoms in the ensemble. A well-known theory of N two-level atoms interacting with a light field was first developed by Dicke [28]. The theory is very effective in the case where only two atoms are involved. An application of two-atom Dicke's model to laser cooling has been reported by Smith and Burnett [29]. However, if the atomic number N in the atomic ensemble is very large, Dicke's model is no longer an effective method since a direct solution of the N-body problem is impractical. Particularly it is difficult to modify the model to include the behavior of the atoms in the ultracold regime.

To formulate a general theory for a many-atom ensemble including the quantum statistics in the ultracold regime, one must resort to other techniques, and we employ quantum field theory in this paper. Owing to the presence of light waves, the internal transition of atoms are involved. Hence the conventional scalar quantum field theory must be extended to including the internal levels of atoms. For simplicity, in this paper, the ultracold atomic ensemble is described as a two-component vector quantum field $\psi(\mathbf{r})=\psi_1(\mathbf{r})|1\rangle+\psi_2(\mathbf{r})|2\rangle$. The state vectors $|1\rangle$ and $|2\rangle$ denote the internal ground state and excited state of the atomic quantum field. The Hermite conjugate components $\psi_j(\mathbf{r})$ and $\psi_j^\dagger(\mathbf{r})$ of the quantum field $\psi(\mathbf{r})$ describe the annihilation and creation of the atoms with the internal state $|j\rangle$ $(j=1,2)$ at position $\mathbf{r}$. The ideal two-level model for the atomic quantum field is a simplified treatment for the real electric dipole transitions. Although in the real cases, both the ground state $|1\rangle$ and the excited state $|2\rangle$ are usually composed of many sublevels, the ideal two-level model can be considered as a reasonable approximation and a useful tool in studying the interaction of atoms with light waves. A general extension of the methods developed in this paper to including the multiple-sublevel structures of atoms is straightforward and will be left for a further publication.

After introducing the vector quantum field, the systematic Hamiltonian for the ensemble composed of many two-level ultracold atoms, the laser field, and the vacuum electromagnetic field can be written as [23,24]

$$H_{\rm sys}=\sum_{j=1}^{2}\int d^3r\,\psi_j^\dagger(\mathbf{r})\left[\frac{-\hbar^2\nabla^2}{2m}\right]\psi_j(\mathbf{r})+\int d^3r\,\psi_2^\dagger(\mathbf{r})\hbar\omega_a\psi_2(\mathbf{r})+H_L+H_F-\int d^3r\mathbf{J}_{12}\cdot\mathbf{A}\psi_1^\dagger(\mathbf{r})\psi_2(\mathbf{r})$$
$$-\hbar\int d^3r\sum_{k\lambda}g^*_{\mathbf{k}\lambda}B^\dagger_{\mathbf{k}\lambda}e^{-i\mathbf{k}\cdot\mathbf{r}}\psi_2^\dagger(\mathbf{r})\psi_1(\mathbf{r})-\hbar\int d^3r\sum_{\mathbf{k}\lambda}g^*_{\mathbf{k}\lambda}B^\dagger_{\mathbf{k}\lambda}e^{-i\mathbf{k}\cdot\mathbf{r}}\psi_1^\dagger(\mathbf{r})\psi_2(\mathbf{r})+\text{H.c}\,. \tag{2}$$

Hamiltonian (2) is the integral of the single-atom Hamiltonian (1) over the distribution space of the atomic quantum field. In order to take quantum statistics into account, we introduce the following equal-time commutators for atomic quantum field operators:

$$\begin{aligned}&[\psi_i(\mathbf{r}),\psi_j(\mathbf{r}')]_q=[\psi_i^\dagger(\mathbf{r}),\psi_j^\dagger(\mathbf{r}')]_q=0\,,\\&[\psi_i(\mathbf{r}),\psi_j^\dagger(\mathbf{r}')]_q=\delta_{ij}\delta(\mathbf{r}-\mathbf{r}')\,,\end{aligned} \tag{3}$$

where we have used the notation $[A,B]_q=AB-qBA$ with $q=1$ corresponding to Bose-Einstein statistics and $q=-1$ to Fermi-Dirac statistics. On the other hand, the quantized laser field satisfies the commutation relations in the Coulomb gauge [27],

$$\begin{aligned}&[\mathbf{A}_i(\mathbf{r}),\mathbf{A}_j(\mathbf{r}')]=[\mathbf{D}_i(\mathbf{r}),\mathbf{D}_j(\mathbf{r}')]=0\,,\\&[\mathbf{D}_i(\mathbf{r}),\mathbf{A}_j(\mathbf{r}')]=i\delta_{ij}^T(\mathbf{r}-\mathbf{r}')\quad(i,j=x,y,z)\,,\end{aligned} \tag{4}$$

where $\mathbf{D}=-\varepsilon_0\mathbf{E}=-\varepsilon_0\partial\mathbf{A}/\partial t$ is the electric displacement vector with $\mathbf{E}$ the field strength and $\delta_{ij}^T(\mathbf{r}-\mathbf{r}')$ is the transverse delta function. The Hamiltonian (2) and the commutation relations (3) and (4) determine the Heisenberg equations of motion for the atomic quantum field components $\psi_j(\mathbf{r})$, the quantized laser field $\mathbf{E}$, and the vacuum electromagnetic field operator $B_{\mathbf{k}\lambda}$. In the Schrödinger picture they have the following forms [24,27]:

$$\begin{aligned}i\hbar\frac{\partial\psi_1}{\partial t}=&-\frac{\hbar^2\nabla^2}{2m}\psi_1-\boldsymbol{\mu}\cdot\mathbf{E}^{(-)}\psi_2\\&-\hbar\sum_{\mathbf{k}\lambda}g^*_{\mathbf{k}\lambda}B^\dagger_{\mathbf{k}\lambda}(t)e^{-i\mathbf{k}\cdot\mathbf{r}}\psi_2\\&-\hbar\psi_2\sum_{\mathbf{k}\lambda}g_{\mathbf{k}\lambda}e^{i\mathbf{k}\cdot\mathbf{r}}B_{\mathbf{k}\lambda}(t)\,,\end{aligned} \tag{5a}$$

$$\begin{aligned}i\hbar\frac{\partial\psi_2}{\partial t}=&-\frac{\hbar^2\nabla^2}{2m}\psi_2+\hbar\omega_a\psi_2-\boldsymbol{\mu}\cdot\mathbf{E}^{(+)}\psi_1\\&-\hbar\sum_{\mathbf{k}\lambda}g^*_{\mathbf{k}\lambda}B^\dagger_{\mathbf{k}\lambda}(t)e^{-i\mathbf{k}\cdot\mathbf{r}}\psi_1\\&-\hbar\psi_1\sum_{\mathbf{k}\lambda}g_{\mathbf{k}\lambda}e^{i\mathbf{k}\cdot\mathbf{r}}B_{\mathbf{k}\lambda}(t)\,,\end{aligned} \tag{5b}$$

$$\begin{aligned}i\hbar\frac{\partial B_{\mathbf{k}\lambda}}{\partial t}=\hbar\omega_kB_{\mathbf{k}\lambda}-\hbar g^*_{\mathbf{k}\lambda}\Bigg[&\int d^3r\,e^{-i\mathbf{k}\cdot\mathbf{r}}\\&\times\psi_2^\dagger(\mathbf{r},t)\psi_1(\mathbf{r},t)\\&+\int d^3r\,e^{-i\mathbf{k}\cdot\mathbf{r}}\\&\times\psi_1^\dagger(\mathbf{r},t)\psi_2(\mathbf{r},t)\Bigg]\,,\end{aligned} \tag{5c}$$

$$\nabla^2\mathbf{E}^\pm-\frac{1}{c^2}\frac{\partial^2\mathbf{E}^{(\pm)}}{\partial t^2}=\mu_0\frac{\partial^2}{\partial t^2}\mathbf{P}^{(\pm)} \tag{5d}$$

where $\mathbf{E}^{(\pm)}$ is the positive frequency and negative frequency part of the electric field $\mathbf{E}$ and the operator $\mathbf{P}^{(+)}=[\mathbf{P}^{(-)}]^\dagger=\boldsymbol{\mu}\psi_1^\dagger\psi_2$ defines the positive frequency part of the polarization of the ultracold atomic ensemble in the Schrödinger picture. Equations (5a) and (5b) determine the dynamic behavior of the atomic quantum field in the presence of the laser field and the vacuum electromagnetic field. Equation (5c) describes the time evolution of the vacuum electromagnetic field due to spontaneous emission of atoms and Eq. (5d) determines the propagation of laser photons in the presence of the ultracold atomic ensemble. Solving Eq. (5c), one obtains

$$B_{\mathbf{k}\lambda}(t)=\left[B_{\mathbf{k}\lambda}(t_0)+ig^*_{\mathbf{k}\lambda}\int_{t_0}^{t}dt'\int d^3r\,e^{i\omega_kt'-i\mathbf{k}\cdot\mathbf{r}}\psi_2^\dagger(\mathbf{r},t')\psi_1(\mathbf{r},t')+ig^*_{\mathbf{k}\lambda}\int_{t_0}^{t}dt'\int d^3r\,e^{i\omega_kt'-i\mathbf{k}\cdot\mathbf{r}}\psi_1^\dagger(\mathbf{r},t')\psi_2(\mathbf{r},t')\right]e^{-i\omega_kt}\,, \tag{6}$$

where the first term $B_{\mathbf{k}\lambda}(t_0)$ gives the free electromagnetic field operator which describes the vacuum fluctuations and the second and third terms give the fields of the radiation or the scattered fields of the atoms. In the single-atom theory [27], the second term is usually neglected due to the rotating-wave approximation. In our many-atom quantum field theory, this term leads to two-body interaction between different ultracold atoms. Substituting Eq. (6) into Eqs. (5a) and

(5b), and working in the rotating frame with laser frequency ω_L, we obtain the reduced equations of motion for the atomic quantum field:

$$i\hbar\frac{\partial\psi_1}{\partial t}=-\frac{\hbar^2\nabla^2}{2m}\psi_1-\boldsymbol{\mu}\cdot\mathbf{E}^{(-)}\psi_2-\hbar\sum_{\mathbf{k}\lambda}g^*_{\mathbf{k}\lambda}B^\dagger_{k\lambda}(t_0)e^{-i\mathbf{k}\cdot\mathbf{r}+i(\omega_k-\omega_L)t}\psi_2-\hbar\psi_2\sum_{\mathbf{k}\lambda}g_{\mathbf{k}\lambda}e^{i\mathbf{k}\cdot\mathbf{r}-i(\omega_k+\omega_L)t}B_{\mathbf{k}\lambda}(t_0)$$
$$+i\hbar\int d^3r'\int_0^{t-t_0}d\tau[G^{(-)}(\tau,\mathbf{r}-\mathbf{r}')]^*\psi_2^\dagger(\mathbf{r}',t-\tau)\psi_1(\mathbf{r}',t-\tau)\psi_2(\mathbf{r},t)$$
$$-i\hbar\int d^3r'\int_0^{t-t_0}d\tau\, G^{(+)}(\tau,\mathbf{r}-\mathbf{r}')\psi_2(\mathbf{r},t)\psi_2^\dagger(\mathbf{r}',t-\tau)\psi_1(\mathbf{r}',t-\tau)\;, \tag{7a}$$

$$i\hbar\frac{\partial\psi_2}{\partial t}=-\frac{\hbar^2\nabla^2}{2m}\psi_2-\hbar\Delta\psi_2-\boldsymbol{\mu}\cdot\mathbf{E}^{(+)}\psi_1-\hbar\sum_{\mathbf{k}\lambda}g^*_{\mathbf{k}\lambda}B^\dagger_{\mathbf{k}\lambda}(t_0)e^{-i\mathbf{k}\cdot\mathbf{r}+i(\omega_k+\omega_L)t}\psi_1-\hbar\psi_1\sum_{\mathbf{k}\lambda}g_{\mathbf{k}\lambda}e^{ik\cdot\mathbf{r}-i(\omega_k-\omega_L)t}B_{\mathbf{k}\lambda}(t_0)$$
$$-i\hbar\int d^3r'\int_0^{t-t_0}d\tau\, G^{(-)}(\tau,\mathbf{r}-\mathbf{r}')\psi_1(\mathbf{r},t)\psi_1^\dagger(\mathbf{r}',t-\tau)\psi_2(\mathbf{r}',t-\tau)$$
$$+i\hbar\int d^3r'\int_0^{t-t_0}d\tau[G^{(+)}(\tau,\mathbf{r}-\mathbf{r}')]^*\psi_1^\dagger(\mathbf{r}',t-\tau)\psi_2(\mathbf{r}',t-\tau)\psi_1(\mathbf{r},t)\;, \tag{7b}$$

where $G^{(\pm)}(\tau,\mathbf{r}-\mathbf{r}')=\sum_{\mathbf{k}\lambda}|g_{\mathbf{k}\lambda}|^2e^{-i(\omega_k\pm\omega_L)\tau+i\mathbf{k}\cdot(\mathbf{r}-\mathbf{r}')}$ are the photon Green's functions and $\Delta=\omega_L-\omega_a$ is the detuning of the laser frequency from the atomic resonance frequency. In Eqs. (7a) and (7b), the integrals over time depend on the field operators $\psi_j(\mathbf{r}',t-\tau)$ $(j=1,2)$ with the time delay τ. According to the Weisskopf-Wigner radiation theory [27], the radiation fields of atoms have the Markoff property and the effect of the time delay on the atomic quantum field can be neglected. In this case, the delayed quantum field operators can be removed from within the integrals over time τ in Eqs. (7a) and (7b). By rearranging all operators in normal order, we finally obtain the Heisenberg equations of motion for the atomic quantum field operators

$$i\hbar\frac{\partial\psi_1}{\partial t}=-\frac{\hbar^2\nabla^2}{2m}\psi_1-\boldsymbol{\mu}\cdot\mathbf{E}^{(-)}\psi_2+i\hbar\int d^3r' L(\mathbf{r}-\mathbf{r}')\psi_2^\dagger(\mathbf{r}',t)\psi_1(\mathbf{r}',t)\psi_2(\mathbf{r},t)+G_1(\mathbf{r},t)\;, \tag{8a}$$

$$i\hbar\frac{\partial\psi_2}{\partial t}=-\frac{\hbar^2\nabla^2}{2m}\psi_2-\hbar(\Delta+i\gamma/2)\psi_2-\boldsymbol{\mu}\cdot\mathbf{E}^{(+)}\psi_1-i\hbar\int d^3r' L(\mathbf{r}-\mathbf{r}')^*\psi_1^\dagger(\mathbf{r}',t)\psi_2(\mathbf{r}',t)\psi_1(\mathbf{r},t)+G_2(\mathbf{r},t)\;, \tag{8b}$$

where $\gamma=4|\boldsymbol{\mu}|^2\omega_L^3/3\hbar c^3$ is the spontaneous emission rate of a single atom in the ensemble. The usual Lamb level shift of a single atom induced by the vacuum electromagnetic field has been included in the detuning Δ in Eq. (8b). The nonlinear two-body correlation or collision coefficient for excited-state and ground-state atoms has the definition in the Markoff approximation

$$L(\mathbf{r}-\mathbf{r}')=\lim_{t-t_0\to\infty}\int_0^{t-t_0}d\tau\{[G^{(-)}(\tau,\mathbf{r}-\mathbf{r}')]^*-G^{(+)}(\tau,\mathbf{r}-\mathbf{r}')\}$$
$$=\sum_{\mathbf{k}\lambda}\left[\frac{2\pi\omega_k}{\hbar V_e}\right]|\boldsymbol{\mu}\cdot\mathbf{e}_{\mathbf{k}\lambda}|^2\left\{\left[\pi\delta(\omega_k-\omega_L)+\mathrm{P}\frac{i}{\omega_k-\omega_L}\right]e^{-i\mathbf{k}\cdot(\mathbf{r}-\mathbf{r}')}+\mathrm{P}\frac{i}{\omega_k+\omega_L}e^{i\mathbf{k}\cdot(\mathbf{r}-\mathbf{r}')}\right\}\;, \tag{9}$$

where P indicates a principal value. To evaluate the summation over all wave vectors $\mathbf{k}$ of the radiation fields in Eq. (9), we pass to the limit of infinite quantization volume $V_e\to\infty$ in the usual way [19], and then obtain the expressions

$$L(\mathbf{r}-\mathbf{r}')=\gamma[K(\mathbf{r}-\mathbf{r}')/2-iW(\mathbf{r}-\mathbf{r}')] \tag{10a}$$

for

$$K(\mathbf{r}-\mathbf{r}')=\frac{3}{2}\left[\sin^2\theta\frac{\sin\xi}{\xi}+(1-3\cos^2\theta)\left[\frac{\cos\xi}{\xi^2}-\frac{\sin\xi}{\xi^3}\right]\right]\;, \tag{10b}$$

$$W(\mathbf{r}-\mathbf{r}')=\frac{3}{4}\left[-\sin^2\theta\frac{\cos\xi}{\xi}+(1-3\cos^2\theta)\left[\frac{\sin\xi}{\xi^2}+\frac{\cos\xi}{\xi^3}\right]\right]\;, \tag{10c}$$

where we define $\xi=|\mathbf{k}_L\cdot(\mathbf{r}-\mathbf{r}')|$ and θ is the angle between the dipole moment $\boldsymbol{\mu}$ and the relative coordinate $\mathbf{r}-\mathbf{r}'$. The noise terms in Eqs. (8) are defined as

$$G_j(\mathbf{r},t)=-\hbar[\Gamma_j^\dagger(\mathbf{r},t)\psi_l+\psi_l\Gamma_l(\mathbf{r},t)]\quad(j\neq l=1,2)\;, \tag{11}$$

with the operators $\Gamma_j(\mathbf{r},t)=\sum_{\mathbf{k}\lambda}g_{\mathbf{k}\lambda}B_{\mathbf{k}\lambda}(t_0)e^{-i[\omega_k+(-1)^j\omega_L]t+i\mathbf{k}\cdot\mathbf{r}}$ $(j=1,2)$ giving the effect of vacuum fluctuations on the atomic quantum field. The noise operators $\Gamma_j(\mathbf{r},t)$ satisfy the following random correlations:

$$\langle \Gamma_l(\mathbf{r},t)\Gamma_j(\mathbf{r}',t')\rangle = \langle \Gamma_l^\dagger(\mathbf{r},t)\Gamma_j(\mathbf{r}',t')\rangle = 0 \; ,$$

$$\langle \Gamma_l(\mathbf{r},t)\Gamma_j^\dagger(\mathbf{r}',t')\rangle = \sum_{\mathbf{k}\lambda}\{|g_{\mathbf{k}\lambda}|^2 e^{-i[\omega_k+(-1)^l\omega_L](t-t')+i\mathbf{k}\cdot(\mathbf{r}-\mathbf{r}')}\}\delta_{jl}$$

$$= \begin{cases} G^{(-)}(t-t',\mathbf{r}-\mathbf{r}') & (j=l=1) \\ G^{(+)}(t-t',\mathbf{r}-\mathbf{r}') & (j=l=2) \\ 0 & (j\neq l=1,2). \end{cases} \qquad (12)$$

The bracket "⟨ ⟩" denotes an average over the vacuum states of the free electromagnetic field. In the Markoff approximation, the above correlations are identical to those of "white noises" [27].

The nonlinear stochastic Schrödinger equations (8) and the quantum propagation equation (5d) determine the collective dynamics of a two-level ultracold atomic ensemble in a laser field. In addition, they form the basis to construct a formalism of nonlinear atom optics for an ultracold atomic beam. The nonlinear terms in Eqs. (8), which originate from the interaction of the ultracold atoms with the vacuum electromagnetic field, describe the many-body collective correlation between ultracold atoms. These terms show that the interaction of the atoms with the photons of vacuum fields leads to a direct interaction between the atoms. This case is very similar to that of electrons interacting with phonons of lattice vibration fields in a superconductor [30]. The real part $\gamma K(\mathbf{r}-\mathbf{r}')$ of the nonlinear correlation coefficient $L(\mathbf{r}-\mathbf{r}')$ accounts for the dissipation of the atomic quantum field due to collisions caused by many-atom spontaneous emission. The imaginary part $-\gamma W(\mathbf{r}-\mathbf{r}')$ corresponds to the interatom interaction potential, which is the result of photon exchanges between the ultracold atoms via the vacuum fields. In terms of Eqs. (10), the correlation coefficient $L(\mathbf{r}-\mathbf{r}')$ has a sharp peak when the interatom distance is close to the atomic resonance wavelength. Hence it determines a long-range correlation of ultracold atoms in the range of atomic resonance wavelengths.

III. FORMALISM OF NONLINEAR ATOM OPTICS

Equations (8) and (5d) describe the general dynamic behavior of ultracold atoms in a laser field. They are applicable to both bosonic atoms and fermionic atoms. In this section, we apply them to construct a basic formalism of nonlinear atom optics for an ultracold atomic beam composed only of bosonic atoms. This assumes that the atomic beam is prepared in an ultracold quantum state where bosonic atoms lose their individual identities. Due to optical excitation, the atoms in a laser field are either in the excited state or in the ground state. However, only the atoms, which remain in the ground state after the interaction with the laser field, can transport spatial coherence at large distances [31]. This condition is realized when the interaction of atoms with laser field is in the adiabatic regime where the interaction time τ_0 is longer than the characteristic time $[\max(\Delta,\gamma)]^{-1}$. In this case, the excited-state component of the atomic quantum field in Eq. (8b) has the adiabatic solution [16,31]

$$\psi_2(\mathbf{r}) \approx -\frac{\Omega^{(+)}}{2(\Delta+i\gamma/2)}\psi_1(\mathbf{r}) - \frac{i}{\Delta+i\gamma/2}\int d^3r' L(\mathbf{r}-\mathbf{r}')^*\psi_1^\dagger(\mathbf{r}')\psi_2(\mathbf{r}')\psi_1(\mathbf{r}) + \frac{G_2}{\hbar(\Delta+i\gamma/2)} \; , \qquad (13)$$

where we have defined the Rabi frequency $\Omega^{(\pm)} = 2\boldsymbol{\mu}\cdot\mathbf{E}^{(\pm)}/\hbar$.

Substituting (13) into Eq. (8a) and neglecting the higher-order terms $O[(\Delta^2+\gamma^2/4)^{-3/2}]$ in the adiabatic regime, we have the reduced equation for the ground-state atomic quantum field operator ψ_1,

$$i\hbar\frac{\partial\psi_1}{\partial t} = \left[-\frac{\hbar^2\nabla^2}{2m} + V(\mathbf{r}) + V_R(\mathbf{r})\right]\psi_1 + \int d^3r' Q(\mathbf{r},\mathbf{r}')\psi_1^\dagger(\mathbf{r}',t)\psi_1(\mathbf{r}',\tau)\psi_1(\mathbf{r},t) \; . \qquad (14)$$

The effective single-particle potential $V(\mathbf{r})$ and the interatom interaction potential $Q(\mathbf{r},\mathbf{r}')$ have the following expressions:

$$V(\mathbf{r}) = \frac{\hbar|\Omega^{(+)}|^2}{4(\Delta+i\gamma/2)} \; , \qquad (15a)$$

$$Q(\mathbf{r},\mathbf{r}') = \frac{i\hbar}{4(\Delta^2+\gamma^2/4)}\left[L(\mathbf{r}-\mathbf{r}')\Omega^{(+)}(\mathbf{r})\Omega^{(-)}(\mathbf{r}') + \frac{\gamma/2+i\Delta}{\gamma/2-i\Delta}L(\mathbf{r}-\mathbf{r}')^*\Omega^{(-)}(\mathbf{r})\Omega^{(+)}(\mathbf{r}') - \frac{|L(\mathbf{r}-\mathbf{r}')|^2}{\gamma/2-i\Delta}|\Omega^{(+)}(\mathbf{r}')|^2\right] . \qquad (15b)$$

The single-particle potential (15a) is the usual dipole potential in the single-atom diffraction theory in the adiabatic approximation [16,31]. In addition to the single-atom dipole potential and the interatom interaction potential, Eq. (14) includes a random potential with the form

$$V_R(\mathbf{r}) \equiv \frac{1}{2(\Delta+i\gamma/2)} \times \{\hbar\Omega^{(-)}[\Gamma_1(\mathbf{r},t)+\Gamma_2^\dagger(\mathbf{r},t)]+\text{H.c.}\}\ , \tag{16}$$

which is due to vacuum fluctuations coupling into the ensemble in the spontaneous emission process of the atoms. In terms of Eq. (14), the vacuum fluctuations are equivalent to a random scattering source of atoms with the statistical average $\langle V_R(\mathbf{r})\rangle=0$. The higher-order statistical properties of the random-scattering source are determined by the random correlation functions (12).

In addition, the single-particle potential $V(\mathbf{r})$ is non-Hermitian due to spontaneous-emission decay. The interatom interaction potential $Q(\mathbf{r},\mathbf{r}')$ is the result of our many-particle quantum field theory. It originates from the photon scattering during spontaneous emission and the photon exchange between the atoms via the vacuum fields. It is evident that the interatom interaction leads to a nonlinearity of the ultracold atomic beam in the laser field. Such a nonlinearity results in a many-body correlation which changes the propagation properties of the ultracold atomic beam. The interatom potential $Q(\mathbf{r},\mathbf{r}')$ is also non-Hermitian with the real part determining the interatom interaction energy due to photon exchanges and the imaginary part giving the loss rate of atoms due to many-body collisions induced by photon scattering.

So far, we have only discussed the origin of atomic nonlinearity due to photon scattering and exchanges in the spontaneous emission process. Below we will show that the absorption and dispersion of laser photons are also an important source of atomic nonlinearity. In terms of Eq. (5d), the interaction of atoms with laser photons results in the change of the propagation properties of the laser field. In the adiabatic regime of atomic motion, substituting Eq. (13) into Eq. (5d) and neglecting the higher-order nonlinear absorption terms, we obtain the quantum propagation equation for the laser field in the rotating frame with laser frequency,

$$\nabla^2\Omega^{(+)}+k_L^2\Omega^{(+)}=2\sigma k_L(\Delta/\gamma-i/2)\psi_1^\dagger(\mathbf{r})\psi_1(\mathbf{r})\Omega^{(+)}\ , \tag{17}$$

where $\sigma=\gamma^2/(4\Delta^2+\gamma^2)\sigma_{\text{peak}}$ is the absorption cross section of the atoms and $\sigma_{\text{peak}}=2|\boldsymbol{\mu}_{12}|^2\omega_L/\hbar\gamma c\varepsilon_0=3\lambda_L^2/2\pi$ is the peak absorption cross section of the atoms. In the above expressions, k_L and λ_L denote the wave number and wavelength of the laser field. The right-hand side of Eq. (17) is the polarization of the ultracold atomic ensemble in the adiabatic approximation. The real part of the polarization induces dispersion of photons and the imaginary part results in absorption of photons. To solve Eq. (17), we consider a standing-wave laser which is composed of two counterpropagating traveling waves (see Fig. 1). In this case, we can express the Rabi frequency as

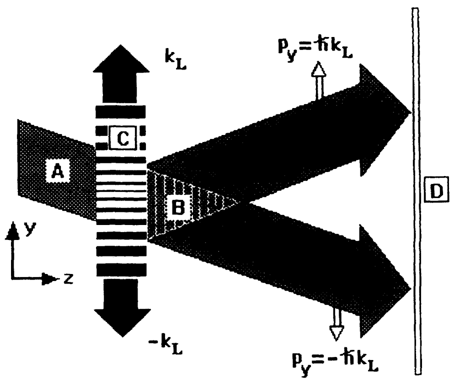

FIG. 1. The schematic diagram for Bragg scattering of an atomic beam by a standing-wave laser beam: A denotes the incident atomic beam, B the near-field interference region, C the standing-wave laser beam, and D the detection screen.

$$\Omega^{(+)}(\mathbf{r})=\Omega_y^{(+)}(\mathbf{r})\exp(ik_Ly)+\Omega_{-y}^{(+)}(\mathbf{r})\exp(-ik_Ly)\ . \tag{18}$$

In the slowly varying envelope approximation, Eqs. (17) and (18) give the propagation equations for the laser field propagating along the $+y$ axis,

$$\frac{\partial\Omega_y^{(+)}}{\partial y}=-\left[\frac{1}{2}+i\frac{\Delta}{\gamma}\right]\sigma\psi_1^\dagger\psi_1\Omega_y^{(+)} \tag{19a}$$

and for the laser field along the $-y$ axis,

$$\frac{\partial\Omega_{-y}^{(+)}}{\partial y}=\left[\frac{1}{2}+\frac{i\Delta}{\gamma}\right]\sigma\psi_1^\dagger\psi_1\Omega_{-y}^{(+)}\ . \tag{19b}$$

In the derivation of Eqs. (19), we ignore the variation of transverse spatial structure of the laser field in the slowly varying approximation. By solving Eqs. (19), we obtain the corrected Rabi frequency due to absorption and dispersion of photons,

$$|\Omega^{(+)}(\mathbf{r})|^2=\frac{1}{4}\Omega(\mathbf{r})^2\left[\exp\left[-\sigma\int_{-\infty}^{y}\psi_1^\dagger\psi_1dy'\right]+\exp\left[-\sigma\int_{y}^{\infty}\psi_1^\dagger\psi_1dy'\right]+2\exp\left[-\frac{1}{2}\sigma\int_{-\infty}^{\infty}\psi_1^\dagger\psi_1dy'\right]\cos\left[2k_Ly-\frac{\Delta}{\gamma}\sigma\int_{-y}^{y}\psi_1^\dagger\psi_1dy'\right]\right]\ , \tag{20}$$

where $\Omega(\mathbf{r})=\Omega_0F(x,z)$ with Ω_0 denoting the peak Rabi frequency and $F(x,z)=\exp[-(x^2+z^2)/2W_L^2]$ is the transverse profile of the two counterpropagating laser fields at $y=-\infty$ and $y=\infty$ which are assumed to have identical transverse profiles to form a standing-wave laser. In terms of Eqs. (14), (15), and (20), it is evident that the absorption and dispersion of laser photons lead to an atomic nonlinearity as well. The atomic nonlinearity due to absorption and dispersion has a more complicated form than that due to spontaneous emission.

Equations (14)–(16) and (20) form the basis of nonlinear atom optics in the adiabatic regime. In this paper, we will consider diffraction of atoms by a standing-wave laser in atom optics. Before discussing the nonlinear diffraction, we analyze the effects of the absorption and dispersion of laser photons.

IV. ATOMIC NONLINEARITY DUE TO ABSORPTION AND DISPERSION

In terms of expression (20), the absorption and dispersion of laser photons result in spatial distortion of the laser field. Such a distortion depends on the spatial distribution of the incident atomic beam. For a low-density atomic beam with $\sigma\int_{-\infty}^{\infty}\psi_1^\dagger\psi_1 dy' \ll 1$, the spatial distortion of the laser field due to absorption and dispersion can be neglected. However, for an ultracold atomic beam, one must evaluate the effects of absorption and dispersion. As an approximate analysis, we replace the atomic quantum field by its initial density distribution with the form

$$\psi_1^\dagger\psi_1 \sim \rho_0 \exp\left[-\frac{y^2}{w_y^2}\right], \tag{21}$$

where ρ_0 is the peak density of the incident atomic beam and w_y is its width in the y direction. We assume that the widths of the incident atomic beam in the x and z direction are much larger than that in the y direction and ignore the spatial variation of the incident atomic beam in the x and z direction. Substituting the initial density distribution (21) into Eq. (20), we have

$$|\Omega^{(+)}(\mathbf{r})|^2=\frac{1}{4}\Omega(\mathbf{r})^2\left\{\exp\left[-\frac{\sqrt{\pi}}{2}\sigma w_y\rho_0[1+\operatorname{erf}(y/w_y)]\right]+\exp\left[-\frac{\sqrt{\pi}}{2}\sigma w_y\rho_0[1-\operatorname{erf}(y/w_y)]\right]\right.$$
$$\left.+2\exp\left[-\frac{\sqrt{\pi}}{2}\sigma w_y\rho_0\right]\cos\left[2k_Ly-\sqrt{\pi}\frac{\Delta}{\gamma}\sigma w_y\rho_0\operatorname{erf}(y/w_y)\right]\right\}. \tag{22}$$

In terms of Eqs. (22) and (15a), we numerically calculate the dipole potential $V(\mathbf{r})$ as shown in Figs. 2–4, where the dipole potential is normalized by a complex constant. Figure 2 is the result for a very small absorption with the condition $(\sqrt{\pi}/2)\sigma w_y\rho_0 \ll 1$. In this case, the dipole potential exhibits periodic structure with period $\lambda_L/2$. However, for a large absorption with $(\sqrt{\pi}/2)\sigma w_y\rho_0 > 1$, the dipole potential is distorted. We show the distorted dipole potential in Figs. 3 and 4 for different values of the detuning. Considering the spatial symmetry in the y direction, the dipole potential is only plotted in the region $y \geq 0$. Figure 3 corresponds to a negative detuning and Fig. 4 corresponds to a positive one. In both cases, the absorption of laser photons in the regions where the atomic beam passes through the laser beam results in the reduction of the height of the dipole potential. Such a reduction is due to the weakening of the laser intensity in the absorption regions. On the other hand, we see that the spatial oscillation period of the dipole potential depends on the sign of the detuning. The negative detuning results in a decrease of the spatial oscillation period and the positive one results in its increase. In terms of Eq. (22), the spatial oscillation period of the dipole potential can qualitatively be expressed as

$$T=\frac{\pi}{k_L-(\Delta/\gamma)[(\sqrt{\pi}/2)\sigma w_y\rho_0]\operatorname{erf}(y/w_y)y^{-1}}. \tag{23}$$

In expression (23), the wave number k_L of the laser field is changed by a factor which is proportional to the detuning Δ and the atomic density distribution. The changing of the wave number of the laser field is due to the dispersion of photons which is caused when the atomic beam passes through the laser. The dispersion induces a phase shift of the laser field which results in a modification of

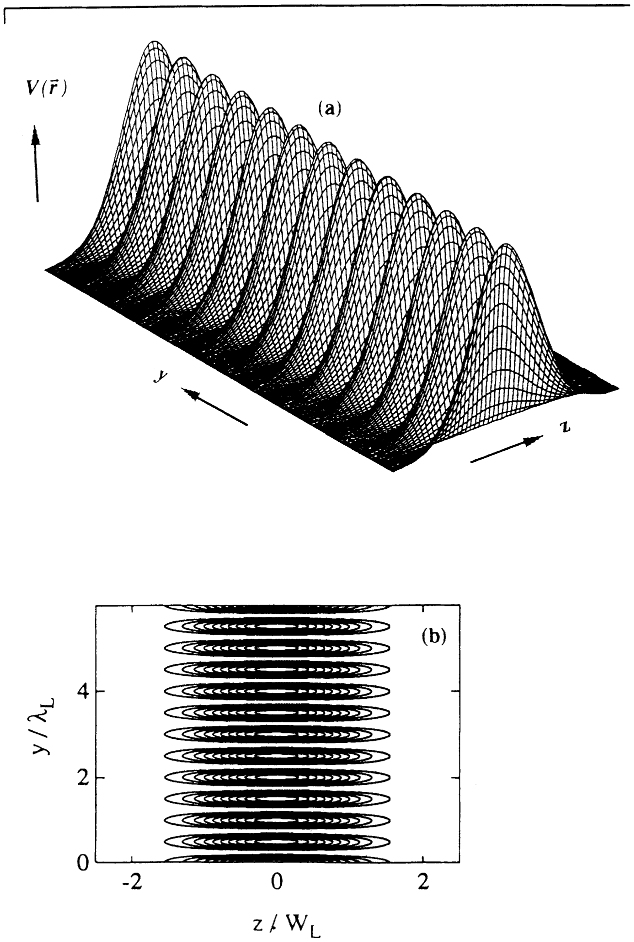

FIG. 2. The dipole potential $V(\mathbf{r})$ for a negligible absorption and dispersion $[(\sqrt{\pi}/2)\sigma w_y\rho_0=0.01]$: (a) the spatial structure of the dipole potential, and (b) the contour of the dipole potential in the y-z plane. The detuning chosen are $\Delta=\pm 10\gamma$.

the spatial oscillation period of the dipole potential. Such a spatial modification tends to destroy the "perfect" periodic structure of the dipole potential.

In terms of the above discussions and Eq. (20), the absorption and dispersion of laser photons depend on the spatial distribution of the atomic beam. Evidently a large absorption and dispersion could seriously change the spatial shape of a standing-wave laser and distort its "perfect" periodic structure as shown in Figs. 3 and 4. Therefore the standing-wave laser is no longer a perfect diffraction grating for an ultracold atomic beam. To avoid the distortion of the laser beam and to observe effective diffraction, one must reduce the absorption and dispersion of laser photons as much as possible. According to Eq. (22), the condition $(\sqrt{\pi}/2)\sigma w_y \rho_0 \ll 1$ is required for an effective diffraction. This gives a limit to the laser parameters such as the detuning, and the atomic parameters such as the peak absorption cross section, the width, and the density of the atomic beam. As an example, we consider the ultracold regime where the interatomic distance is close to the atomic resonance wavelength and the atomic density approximately satisfies $\rho_0 \lambda_L^3 \sim 1$. In this case, the detuning must satisfy the condition $\Delta \gg (\gamma/4)\sqrt{3w_y/\sqrt{\pi}\lambda_L}$ for negligible absorption and dispersion.

On the other hand, the spontaneous emission of atoms results in the dissipation and random fluctuations of atoms in the laser field which cause random scattering of atoms and destroy the coherence of the atomic beam. Hence to avoid the effects of dissipation and random fluctuations due to the spontaneous emission of atoms, a large detuning is also a necessary condition.

In this paper, our main purpose is to present the basic ideas of atomic nonlinearity and its role in nonlinear atom optics. Hence at this stage we wish to eliminate dissipation and random fluctuations due to spontaneous emission of the atoms. This is achievable in the off-resonance regime. Meanwhile, absorption and dispersion

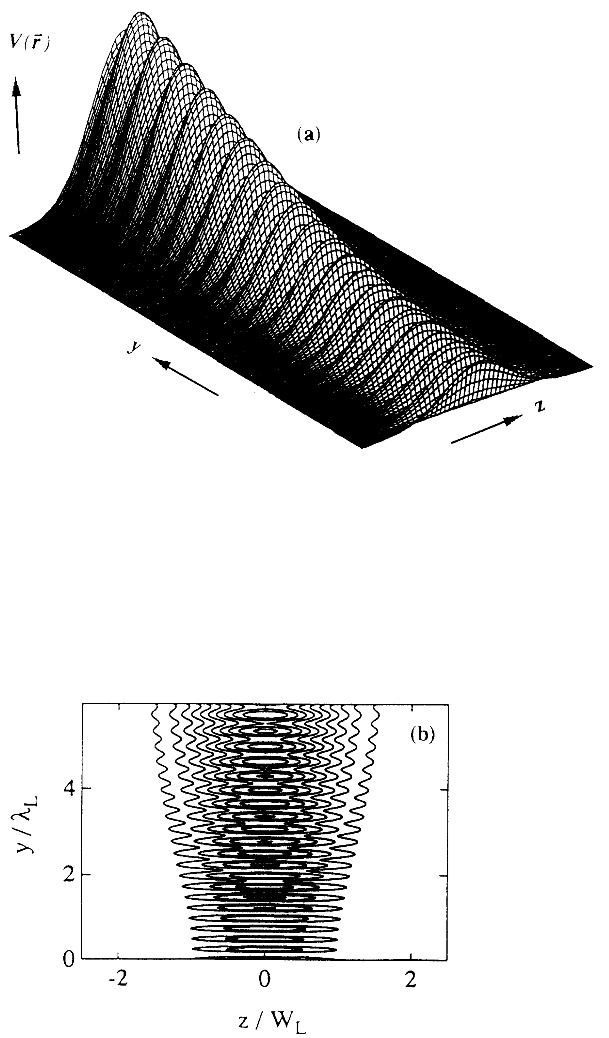

FIG. 3. The dipole potential $V(\mathbf{r})$ for a negative detuning $\Delta = -10\gamma$ and a large absorption and dispersion $[(\sqrt{\pi}/2)\sigma w_y \rho_0 = 3]$: (a) the spatial structure of the dipole potential, and (b) the contour of the dipole potential in the y-z plane.

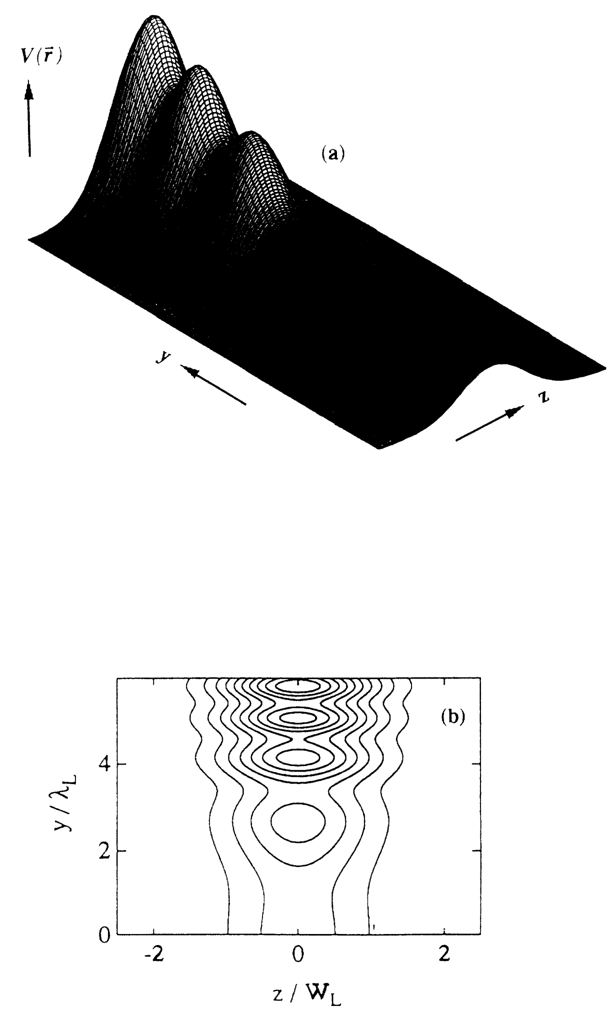

FIG. 4. The dipole potential $V(\mathbf{r})$ for a positive detuning $\Delta = 10\gamma$ and a large absorption and dispersion $[(\sqrt{\pi}/2)\sigma w_y \rho_0 = 3]$: (a) the spatial structure of the dipole potential, and (b) the contour of the dipole potential in the y-z plane.

is negligible as well in this regime. Then the atomic nonlinearity is mainly due to photon-exchange interaction between atoms.

V. NONLINEAR DIFFRACTION OF ULTRACOLD ATOMIC BEAM

In this section, we concentrate on studying the effects of atomic nonlinearity due to long-range photon-exchange potential $W(\mathbf{r}-\mathbf{r}')$ on diffraction of ultracold atoms in the off-resonance regime. Neglecting absorption and dispersion, we have the Rabi frequency

$$|\Omega^{(+)}(\mathbf{r})|^2=\Omega_0^2\exp\left[-\frac{x^2+z^2}{W_L^2}\right]\cos^2(k_L y)$$

in terms of Eq. (20). Then from Eqs. (14) and (15) we obtain the simplified equation of motion for the ground-state atomic quantum field in a standing-wave laser with dissipation and random fluctuations ignored [24]:

$$i\hbar\frac{\partial\psi_1}{\partial t}=\left[-\frac{\hbar^2\nabla^2}{2m}+\frac{\hbar\Omega_0^2}{4\Delta}\exp\left[-\frac{x^2+z^2}{W_L^2}\right]\cos^2(k_L y)\right]\psi_1 -\hbar\chi\exp\left[-\frac{x^2+z^2}{W_L^2}\right]\cos^2(k_L y)\psi_1^\dagger\psi_1\psi_1\ , \qquad (24)$$

where $\chi=\Omega_0^2\gamma V_c/2\Delta^2$ defines the two-body collision rate of ultracold atoms in the adiabatic regime of atomic motion and $V_c=|\int W(\mathbf{r})d^3\mathbf{r}|$ gives the effective scattering volume of atoms due to photon-exchange interaction. In the derivation of Eq. (24), we have used the sharpness of the long-range photon-exchange potential $W(\mathbf{r}-\mathbf{r}')$ in the region of the atomic resonance wavelength. In this case, the Rabi frequency and the atomic quantum field operator can be considered as spatial slowly varying functions and removed from within the integrals in (14).

The physics implicit in Eq. (24) is very clear. The standing-wave laser induces a periodic atomic potential along the y axis. The nonlinear term depends on the density of the atomic beam and the two-body collision rate χ which plays a similar role to that of a nonlinear optical susceptibility of a Kerr-type medium in conventional nonlinear optics. The density of the atomic beam plays the role of the intensity of light in conventional optics. By analogy with the conventional nonlinear optics, Eq. (24) is similar to that of a light wave propagating in a nonlinear periodic dielectric medium. Therefore we see that atoms and photons exchange their role in conventional nonlinear optics. In other words, the light wave just acts as a nonlinear "medium" for an ultracold atomic beam in nonlinear atom optics.

To simplify our discussions, we study a typical example in atom optics where the incident atomic beam propagates along the z axis with momentum vector ($p_{x0}=0,p_{y0}=\hbar K_{0y},p_{z0}=\hbar K_{0z}$) and kinetic energy E. In this example, the width of the incident atomic beam in the x direction is assumed to be wider than that in the y direction and narrower than the width of the laser beam so that one can ignore the propagation of the atomic beam in the x direction. The incident atomic beam is provided by an ultracold atomic source where there are a large number of bosonic atoms condensing in a macroscopic quantum state. In this case, the mean-field approximation is applicable [26,32] and the atomic quantum field operator for the ultracold atomic beam in Eq. (24) can be replaced by a c-number macroscopic wave function $\Phi(\mathbf{r})$.

When the atomic beam passes through the standing-wave laser beam, the periodic structure results in diffraction of the incident atomic beam into many components in the y direction. For stationary propagation, the atomic macroscopic wave function can be expanded in terms of the diffraction modes as follows [23]:

$$\Phi(\mathbf{r})=\left[\sum_{n=-\infty}^{\infty}\Phi_n(y,z)e^{i(K_{0y}+2nk_L)y}\right]e^{iK_{0z}z-iEt/\hbar}\ , \qquad (25)$$

where $\Phi_n(y,z)$ is the spatial slowly varying envelope of the diffracted atomic beams. Substituting (25) into Eq. (24) and neglecting the second derivatives $\partial^2\Phi_n/\partial y^2$, $\partial^2\Phi_n/\partial z^2$ in the slowly varying envelope approximation, we have the equations of motion for the diffracted beams,

$$i\left[\frac{\partial\Phi_n}{\partial\tau}+v_n\frac{\partial\Phi_n}{\partial y}\right]=\omega_n\Phi_n+g(\tau)(2\Phi_n+\Phi_{n-1}+\Phi_{n+1}) +\sum_{jlq}\eta_{njlq}(\tau)\Phi_j^\dagger\Phi_l\Phi_q\ , \qquad (26)$$

where $\tau=v_g^{-1}z$ defines the effective time variable, $v_g=\hbar K_{0z}/m$ is the group velocity of the atomic beam in the z direction, $\omega_n=(n_0+2n)^2\omega_R$ is the de Broglie frequency for nth diffraction mode with $\omega_R=\hbar k_L^2/2m$ defining the single-photon recoil frequency, and $v_n=(n_0+2n)v_R$ is the group velocity of the nth diffracted atomic beam in the y direction with $v_R=\hbar k_L/m$ defining the single-photon recoil velocity. We have noted $n_0=K_{0y}/k_L$ and generally, n_0 need not be an integer. The linear coupling coefficient between different diffracted beams has the definition $g(\tau)=|\Omega_0|^2/16\Delta\exp(-\tau^2/\tau_0^2)$ with $\tau_0=W_L/v_g$ defining the flight time of atoms through the laser beam. The linear coupling coefficient is a time-dependent function due to the transverse Gaussian profile of the laser beam. The nonlinear coupling coefficients have the definitions

$$\eta_{njlq}(\tau)=-\frac{\chi}{4}\exp\left[-\frac{\tau^2}{\tau_0^2}\right]\times(\delta_{j,l+q-n+1}+\delta_{j,l+q-n-1}+2\delta_{j,l+q-n})\ . \qquad (27)$$

Equations (26) are a set of nonlinear coupled wave equations. For a single-atom beam or a low-density atomic beam, Eqs. (26) have identical forms to those in the single-atom diffraction theory [16] with the nonlinear terms negligible. Equations (26) can be further simplified by choosing appropriate resonance conditions. In this paper, we consider the diffraction of atoms in the Bragg resonance regime [16]. The diffraction of a single-atom beam in the Bragg resonance regime has been experimentally demonstrated [16]. To satisfy the Bragg resonance condition, the momentum component of the incident atomic beam in the y direction must be arranged to match one single-photon recoil momentum. Experimentally this can be realized by controlling the angle between the atomic beam and the standing-wave nodes so that the incident momentum $p_{y0}=-m\hbar k_L$. The integer m denotes the diffraction order. For $m=1$ and also $n_0=-1$, one has the first-order Bragg scattering. Higher-order Bragg scattering has similar characters to the first order. Therefore we only need consider the first-order Bragg scattering. In this case, only two diffraction modes with indices $n=0$ and 1 can resonantly couple with each other. Physically, the first-order Bragg resonance corresponds to an absorption and stimulated emission process from the undiffracted $(n_0+2n=-1)$ to the diffracted $(n_0+2n=1)$ momentum eigenmode. Hence for the first-order Bragg scattering we can neglect the higher-order diffraction modes and truncate Eqs. (26) into the following simple forms:

$$i\left[\frac{\partial}{\partial\tau}-v_R\frac{\partial}{\partial y}\right]\Phi_0=\nu(\tau)\Phi_0+g(\tau)\Phi_1+2c(\tau)(\Phi_0^\dagger\Phi_0+2\Phi_1^\dagger\Phi_1)\Phi_0+c(\tau)(2\Phi_0^\dagger\Phi_0+\Phi_1^\dagger\Phi_1)\Phi_1+c(\tau)\Phi_1^\dagger\Phi_0^2\,, \tag{28a}$$

$$i\left[\frac{\partial}{\partial\tau}+v_R\frac{\partial}{\partial y}\right]\Phi_1=\nu(\tau)\Phi_1+g(\tau)\Phi_0+2c(\tau)(\Phi_1^\dagger\Phi_1+2\Phi_0^\dagger\Phi_0)\Phi_1+c(\tau)(2\Phi_1^\dagger\Phi_1+\Phi_0^\dagger\Phi_0)\Phi_1+c(\tau)\Phi_0^\dagger\Phi_1^2\,, \tag{28b}$$

where $\nu(\tau)=\omega_0+2g(\tau)=\omega_1+2g(\tau)$ is the frequency for the two Bragg scattering modes. The nonlinear coupling coefficient is denoted as $c(\tau)=-(\chi/4)\exp(-\tau^2/\tau_0^2)=-\beta g(\tau)$ with $\beta=2\gamma V_c/\Delta$. The macroscopic wave function in Eq. (25) now has the simple form in the Bragg resonance regime

$$\Phi(\mathbf{r})=[\Phi_0(y,z)e^{-ik_Ly}+\Phi_1(y,z)e^{ik_Ly}]e^{iK_{0z}z-iEt/\hbar}\,. \tag{29}$$

Mathematically, Eqs. (28) describe the dynamics of a nonlinear coupler. The well-known examples for a nonlinear coupler are the nonlinear beam splitter in conventional nonlinear optics and the optical coupler in nonlinear guided-wave optics [33]. By analogy with nonlinear optics, the nonlinearity in Eqs. (28) has a similar form to a Kerr-type optical nonlinearity and induces self-phase modulation and cross-phase modulation of atomic waves [25]. Optical self-phase modulation and

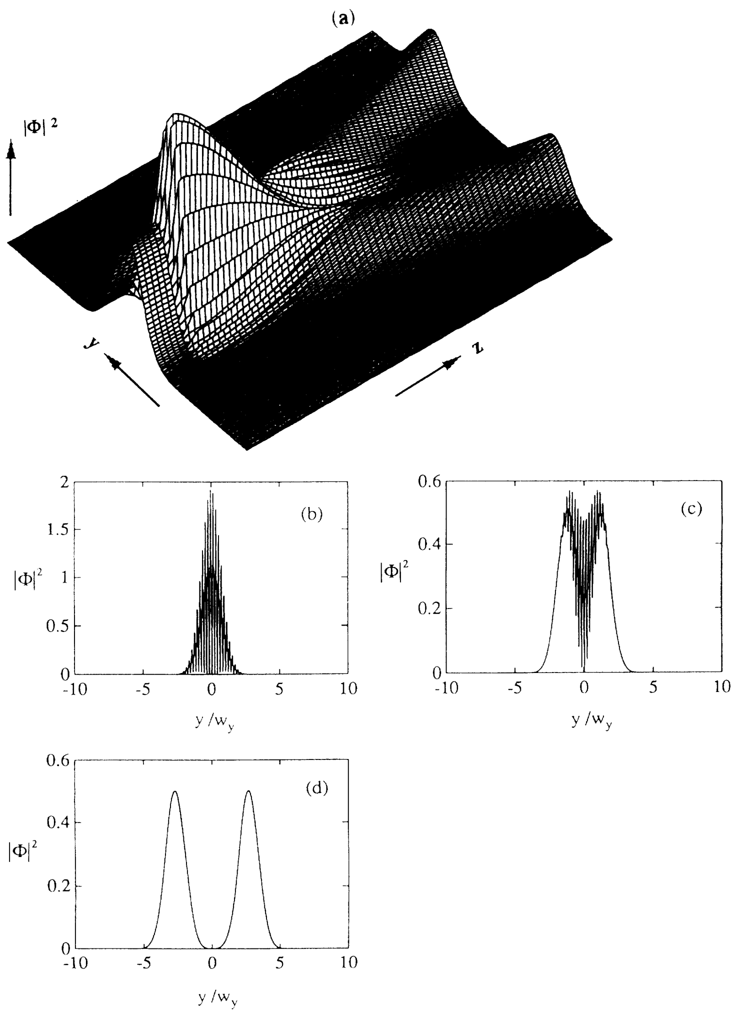

FIG. 5. The density distribution of the atomic beam for linear Bragg scattering. The parameters chosen are $g_0=\pi/4$ and $\beta\rho_0=0.001$. (a) The global density distribution of the atomic beam in propagation, (b) the near-field density distribution with $\tau=2\tau_0$ and the oscillation is due to the near-field interference of the diffracted atomic beams, (c) the near-field density distribution with $\tau=30\tau_0$, and (d) the far-field density distribution with $\tau=60\tau_0$.

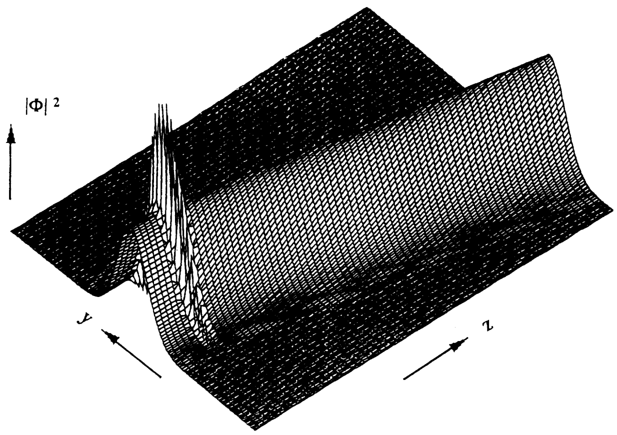

FIG. 6. The global density distribution of the atomic beam for linear Bragg scattering with the parameters chosen as $g_0=\pi$ and $\beta\rho_0=0.001$.

cross-phase modulation are well-known nonlinear phenomena in nonlinear optics. To study the atomic version of these nonlinear phenomena in atom optics, we numerically simulate the propagation of an incident atomic beam it the Bragg resonance regime. The results are discussed below.

VI. NUMERICAL SIMULATION FOR NONLINEAR BRAGG SCATTERING

In this section, we give the numerical analysis for the diffraction of an incident ultracold atomic beam in the Bragg resonance regime. The incident atomic beam is assumed to have a Gaussian density profile with wave vector in the y direction matching the single-photon recoil momentum

$$\Phi_{\text{in}}(y,-\infty)=\sqrt{\rho_0}\exp\left[-\frac{y^2}{2w_y^2}-ik_Ly\right]e^{iR_{0z}z-iEt/\hbar}, \tag{30}$$

where w_y is the beam width in the y direction and $\rho_0=J_0/v_g$ is the density of the atomic beam which is provided by an ultracold atomic source localized at $z=-\infty$. Figure 1 is a schematic diagram for the Bragg scattering of atoms. The atomic source continuously releases the ultracold atomic flow with the rate J_0 which has the equivalent meaning to the light intensity in conventional optics. In terms of Eqs. (29) and (30), we have the initial conditions for Eqs. (28),

$$\Phi_0(y,-\infty)=\sqrt{\rho_1}\exp\left[-\frac{y^2}{2w_y^2}\right], \tag{31a}$$

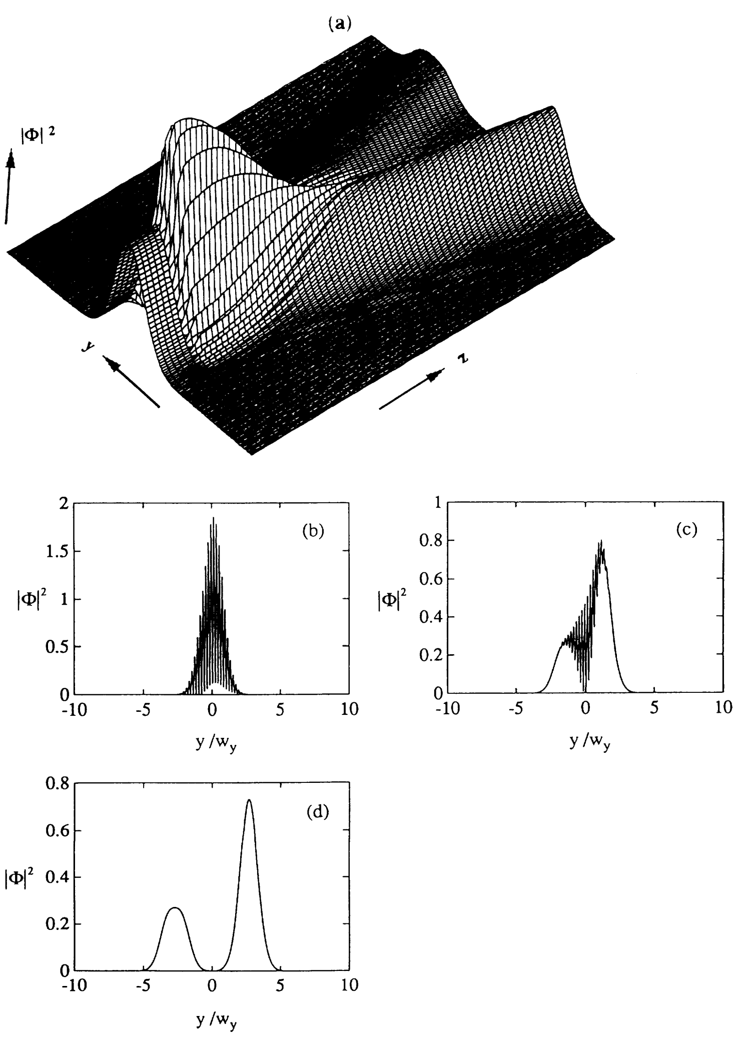

FIG. 7. The density distribution of the atomic beam for nonlinear Bragg scattering. The parameters chosen are $g_0=\pi/4$ and $\beta\rho_0=0.3$. (a) The global density distribution of the atomic beam in propagation, (b) the near-field density distribution with $\tau=2\tau_0$ and the oscillation is due to the near-field interference of the diffracted atomic beams, (c) the near-field density distribution with $\tau=30\tau_0$, and (d) the far-field density distribution with $\tau=60\tau_0$.

$$\Phi_1(y,-\infty)=0 \ . \tag{31b}$$

Under conditions (31), we numerically simulate the spatial propagation of the incident atomic beam in terms of Eqs. (28) and (29). The spatial density distributions are shown in Figs. 5–9. For comparisons, in Figs. 5 and 6, we give the results for a low-density atomic beam with a negligible nonlinearity. The laser parameters in Fig. 5 are chosen to satisfy the condition $g_0 \equiv \int_{-\infty}^{\infty} g(\tau) d\tau = \pi/4$ so that the incident atomic beam splits into two components with identical density profiles. In terms of the results in Fig. 5(a), when the incident atomic beam passes through the laser region, the interaction of the atoms with the laser beam results in the splitting of the initial atomic beam into two coherent beams, respectively, with group velocities $\pm v_R$ in the y direction. In the near-field region, the two coherent components overlap and we see density oscillations due to the interference of the two coherent beams [see Fig. (5b)]. With the increase of propagation distance, the two coherent beams gradually separate and the interference vanishes in the far-field region where we have two fully separated beams with Gaussian profiles as shown in Figs. 5(c) and 5(d) and also in Fig. 5(a). The splitting of the atomic beam is due to the exchange of atoms between two diffraction modes. Such an exchange means that some atoms in the incident beam change their momentum in the y direction. The change of atomic momentum is caused by the mechanical effect induced by the laser beam. The number of exchanged atoms between two diffraction modes depends on the linear coupling strength g_0. When the laser parameters are chosen to give $g_0=\pi$, the exchange of atoms between two diffraction modes experiences a cycle and the atoms are completely diffracted back to the initial incident beam. In this case, the incident beam does not split after interaction with the laser (see Fig. 6). The above results show that the exchange of atoms in diffraction exhibits a periodic character [16] in the absence of atomic nonlinearity.

However, for an ultracold atomic beam with high density, the nonlinearity is important and the diffraction of atoms will be affected by it. In Fig. 7, we choose the same linear coupling strength g_0 as used in Fig. 5. Compared to Fig. 5, the atomic nonlinearity causes a splitting of the incident atomic beam into two components with different density profiles. Similarly, we simulate the case where the laser parameters are chosen the same as in Fig. 6 with $g_0=\pi$. The results are displayed in Fig. 8. We find that including the atomic nonlinearity, the incident atomic beam coherently splits into two components and

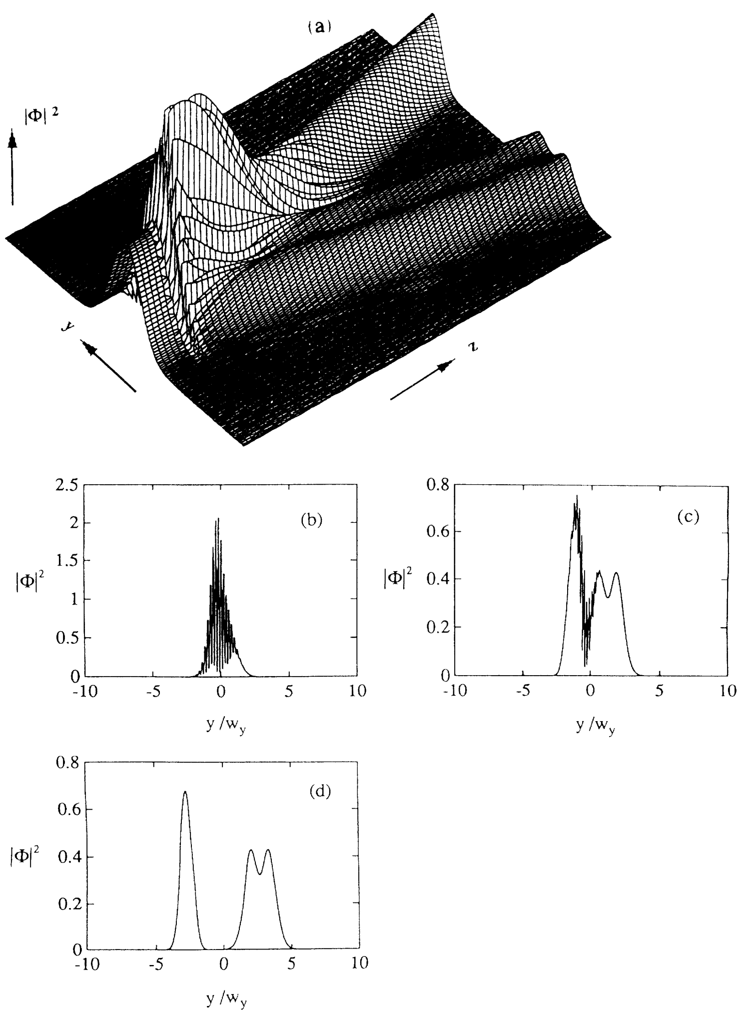

FIG. 8. The density distribution of the atomic beam for nonlinear Bragg scattering. The parameters chosen are $g_0=\pi$ and $\beta\rho_0=0.3$. (a) The global density distribution of the atomic beam in propagation, (b) the near-field density distribution with $\tau=2\tau_0$ and the oscillation is due to the near-field interference of the diffracted atomic beams, (c) the near-field density distribution with $\tau=30\tau_0$, and (d) the far-field density distribution with $\tau=60\tau_0$.

one of the split components exhibits two-peak structure in the far-field region. To understand the phenomena, we seek approximately analytical solutions of Eqs. (28) by neglecting the spatial propagation of the beam in the y direction. We find the approximate solutions of Eqs. (28) in the form,

$$|\Phi_0(y,z)|^2=|\Phi_{in}(y,-\infty)|^2\cos^2[\theta(\tau)+\Delta\theta(y,\tau)] , \quad (32a)$$

$$|\Phi_1(y,z)|^2=|\Phi_{in}(y,-\infty)|^2 \sin^2[\theta(\tau)+\Delta\theta(y,\tau)] , \quad (32b)$$

where

$$\theta(\tau)=\int_{-\infty}^{\tau} g(\tau)d\tau=\frac{g_0}{2}\left[1+\operatorname{erf}\left[\frac{\tau}{\tau_0}\right]\right]$$

is the phase shift due to the linear coupling. The nonlinearity induces an additional phase shift

$$\Delta\theta(y,\tau)=-\beta\theta(\tau)\{|\Phi_{in}(y,-\infty)|^2 +\tfrac{1}{2}[\Phi_0^\dagger(y,z)\Phi_1(y,z) +\Phi_1^\dagger(y,z)\Phi_0(y,z)]\} .$$

In the far-field region $z\to\infty$, the phase shift due to linear coupling is a constant $\theta(\infty)=g_0$ and the nonlinear phase shift $\Delta\theta(y,\infty)$ is still a function of the spatial coordinate y and depends on the transverse distribution of the atomic beam. Hence the nonlinear phase shift is nonuniform in the y direction. Such a nonuniform phase shift modulates the spatial distributions of the split atomic beams and causes the multiple-peak structures in the density profiles. As an example, we consider the case shown in Fig. 8 where $\theta(\infty)=g_0=\pi$, and the far-field atomic densities of the diffracted beams have the forms

$$|\Phi_0(y,\infty)|^2=|\Phi_{in}(y,-\infty)|^2\cos^2[\Delta\theta(y,\infty)] , \quad (33a)$$

$$|\Phi_1(y,\infty)|^2=|\Phi_{in}(y,-\infty)|^2\sin^2[\Delta\theta(y,\infty)] . \quad (33b)$$

For a negligible nonlinearity, the nonlinear phase shift $\Delta\theta(y,\infty)\simeq 0$ and we have $|\Phi_0(y,\infty)|^2=|\Phi_{in}(y,-\infty)|^2$ and $|\Phi_1(y,\infty)|^2=0$. Hence the incident beam does not split in this case. However, it is evident that a large nonlinearity results in a nonzero nonlinear phase shift $\Delta\theta(y,\tau)$ which causes splitting of the incident beam and also causes a nonuniform spatial modulation of the split beams in terms of Eqs. (33). Hence the nonuniform phase modulation due to atomic nonlinearity plays an important role in the propagation of ultracold atomic beams. In Fig. 9, we give a further simulation for a larger linear coupling strength $g_0=2\pi$. We see that the density profiles of the diffracted beams are further changed due to the nonlinear phase modulation.

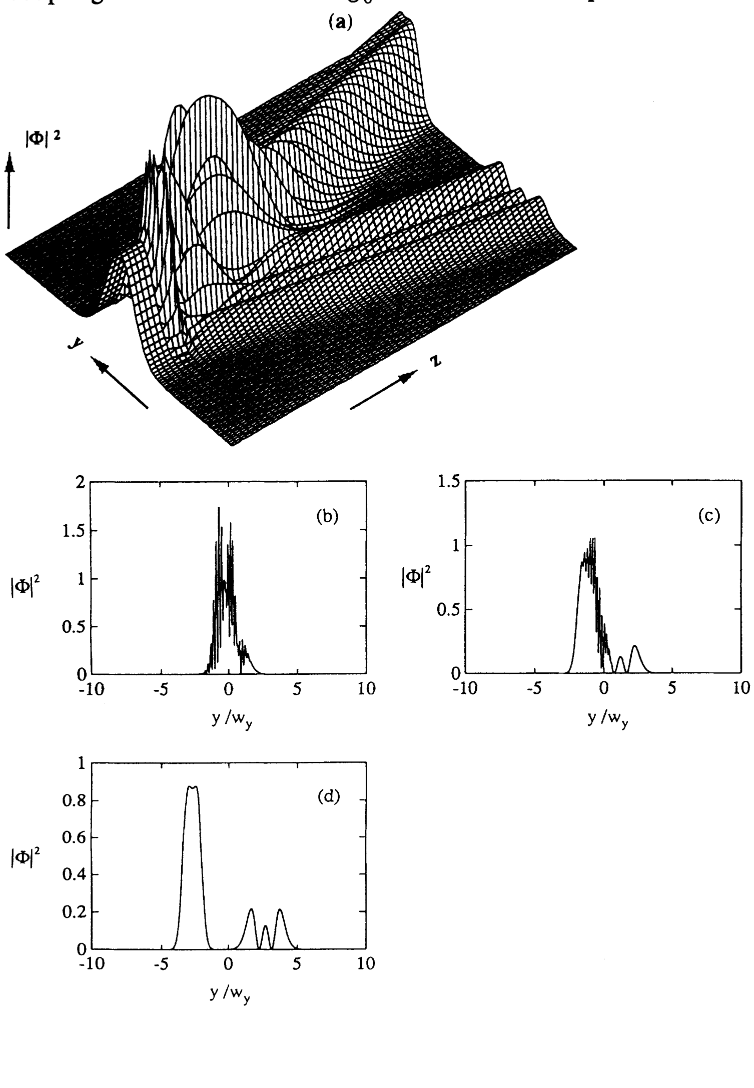

FIG. 9. The density distribution of the atomic beam for nonlinear Bragg scattering. The parameters chosen are $g_0=2\pi$ and $\beta\rho_0=0.3$. (a) The global density distribution of the atomic beam in propagation, (b) the near-field density distribution with $\tau=2\tau_0$ and the oscillation is due to the near-field interference of the diffracted atomic beams, (c) the near-field density distribution with $\tau=30\tau_0$, and (d) the far-field density distribution with $\tau=60\tau_0$.

TABLE I. The atomic parameters for the observation of nonlinear effects in atom optics. The critical density $\rho_0 \sim \lambda_L^{-3}$ and the critical temperature $T \sim 2\pi\hbar^2/mk_B\lambda_L^2$.

Atom	Mass (a.m.u.)	Selected transition	Transition wavelength (Å)	Critical density (cm^{-3})	Critical temperature (μK)
${}^1_1$H	1.0078	$2S_{1/2}$-$3P_{1/2}$	6562.74	3.54×10^{12}	7.0
${}^{23}_{11}$Na	22.990	$3S_{1/2}$-$3P_{3/2}$	5889.95	4.89×10^{12}	0.38
${}^{85}_{37}$Rb	84.912	$5S_{1/2}$-$5P_{3/2}$	7800.27	2.1×10^{12}	0.059
${}^{133}_{55}$Cs	132.91	$6S_{1/2}$-$6P_{3/2}$	8521.12	1.6×10^{12}	0.03

VII. CONCLUSIONS

In this paper, we develop a systematic theory for the interaction of ultracold atoms with a laser field in the framework of vector quantum field theory. Both the atoms and the laser field are treated as a quantum field. A vector stochastic nonlinear Schrödinger equation for ultracold atoms and a quantum propagation equation for laser photons are derived. These equations form the basis to study many-body quantum statistics and atomic nonlinearity in atom optics. As a straightforward application of the theory, we construct a formalism of nonlinear atomic optics for an ultracold atomic beam. Applying the formalism to the diffraction of an ultracold atomic beam by a standing-wave laser, we find that the photon exchanges between ultracold atoms in the beam induces an effective atomic nonlinearity for the atomic waves which is analogous to an optical Kerr-type nonlinearity for coherent light waves. Such an atomic nonlinearity can result in self-phase modulation and cross-phase modulation of atomic waves. In the Bragg resonance regime, we simulate the propagation of an ultracold atomic beam. The atomic nonlinearity results in spatial modulation of atomic density profiles for the Bragg scattering waves.

In addition, we wish to emphasize that the observation of the nonlinear diffraction of atomic beams requires that the incident atomic beams be provided by an ultracold atomic source which is prepared in the ultracold state. In the languages of quantum statistical theory, the condition for an ultracold atomic beam is that the single-mode degeneracy of bosonic atoms in the beam or the "brightness" of the atomic beam, $N_v=\rho_0\lambda_{dB}^3$, must be larger than one. Here $\rho_0=J_0/v_g$ is the peak density of the atomic beam and $\lambda_{dB}=\sqrt{2\pi\hbar^2/mk_BT}$ is its thermal de Broglie wavelength which determines the spatial coherence of the atomic beam. Under this condition, the thermal de Broglie wavelength λ_{dB} must be comparable with the average interatom distance $\rho_0^{-1/3}$. For photon-exchange interaction which has a characteristic interatom distance close to the atomic resonance wavelength, the thermal de Broglie wavelength must achieve the order of the atomic resonance wavelength, i.e., $\lambda_{dB}\sim\lambda_L$. In this case, the density of the atomic beam must meet the criterion $\rho_0\lambda_L^3>1$. As some numerical examples, we give the critical temperatures and densities of atoms in Table I which are required to observe the atomic nonlinearity induced by photon-exchange interaction. In terms of Table I, an ultracold atomic source is necessary to study nonlinear phenomena in atom optics. This case is just similar to that in nonlinear optics where a high-intensity coherent laser source is required. Techniques are now being developed towards generating ultracold atomic sources with high bosonic degeneracy. Some principles have also been suggested to generate a highly bright coherent atomic beam [12,13].

Finally we point out that although we only discuss the nonlinear diffraction in this paper, the quantum field theory developed here provides a general method which could be applied for wide problems in atom optics, quantum optics, and interaction of light waves with condensed matter. For example, the atomic nonlinearity could result in generation of atomic soliton [26] and self-trapping of atomic beams [34] in laser beams. It is not an exaggeration that almost all nonlinear optical phenomena could find their versions in nonlinear atom optics in terms of the general formalism constructed in this paper. Particularly, the absorption and dispersion of laser photons lead to a complicated form of atomic nonlinearity which would induce new nonlinear phenomena in atom optics when absorption and dispersion are not negligible. In addition, the quantum field theory and the stochastic nonlinear Schrödinger equations present a simple way to study the ultracold collisions of atoms in a laser field, quantum statistics in the ultracold regime, and the critical condition for Bose-Einstein condensation in laser-cooled neutral atomic gases. These open a new window onto future research in laser cooling and atom optics.

ACKNOWLEDGMENTS

The authors thank Barry C. Sanders, G. J. Milburn, and J. D. Cresser for their helpful discussions. W.Z. is grateful for the support of the Australian Research Council. D.F.W. is grateful for the support of New Zealand Foundation of Research Science and Technology, the New Zealand Lotteries Grants Board, and the University of Auckland Research Committee.

[1] S. Chu, J. E. Bjorkholm, A. Ashkin, and A. Cable, Phys. Rev. Lett. **57**, 314 (1986).

[2] M. Prentiss, A. Cable, J. E. Bjorkholm, S. Chu, E. Raab, and D. E. Pritchard, Opt. Lett. **13**, 452 (1988).

[3] D. Sesko, T. Walker, C. Montroe, A. Gallagher, and C. Wieman, Phys. Rev. Lett. **63**, 961 (1989).

[4] P. Lett. P. Jessen, W. Phillips, S. Rolston, C. Westbrook, and P. Gould, Phys. Rev. Lett. **67**, 2139 (1991).

[5] C. Monroe, W. Swann, H. Robinson, and C. Wieman, Phys. Rev. Lett. **65**, 1571 (1990).
[6] J. M. Doyle, J. C. Sandberg, I. A. Yu, C. L. Cesar, D. Kleppner, and T. J. Greytak, Phys. Rev. Lett. **67**, 603 (1991).
[7] See Appl. Phys. B **54** (5) (1992), special issue on atom optics, edited by J. Mlynek, V. Balykin, and P. Meystre.
[8] T. Walker, D. Sesko, and C. Wieman, Phys. Rev. Lett. **64**, 408 (1990).
[9] D. Sesko, T. Walker, and C. Wieman, J. Opt. Soc. Am. B **8**, 946 (1991).
[10] T. J. Greytak and D. Kleppner, in *Trends in Atomic Physics*, edited by G. Grynberg and R. Stora (North-Holland, Amsterdam, 1984).
[11] E. Cornell, C. Monroe, and C. Wieman, Phys. Rev. Lett. **67**, 2439 (1991).
[12] V. Balykin and V. Letokhov, Appl. Phys. B **48**, 517 (1989).
[13] H. Wallis, J. Dalibard, and C. Cohen-Tannoudji, Appl. Phys. B **54**, 407 (1992).
[14] S. Stenholm, Rev. Mod. Phys. **58**, 699 (1986).
[15] C. Tanguy, S. Reynaud, and C. Cohen-Tannoudji, J. Phys. B **17**, 4623 (1984).
[16] P. Martin, B. Oldaker, A. Miklich, and D. Pritchard, Phys. Rev. Lett. **60**, 515 (1988).
[17] E. Arimondo, A. Bambini, and S. Stenholm, Opt. Commun. **37**, 103 (1981).
[18] E. Arimondo, A. Bambini, and S. Stenholm, Phys. Rev. A **24**, 898 (1981).
[19] R. Cook, Phys. Rev. A **22**, 1078 (1980).
[20] R. Graham, D. F. Walls, and P. Zoller, Phys. Rev. A **45**, 5018 (1992).
[21] Weiping Zhang and D. F. Walls, Phys. Rev. Lett. **68**, 3287 (1992).
[22] Weiping Zhang and D. F. Walls, Phys. Rev. A **47**, 626 (1993).
[23] Weiping Zhang and D. F. Walls, Quantum Opt. **5**, 9 (1993).
[24] Weiping Zhang, Phys. Lett. A **176**, 53 (1993).
[25] Weiping Zhang (unpublished).
[26] Weiping Zhang, D. F. Walls, and B. C. Sanders, Phys. Rev. Lett. **72**, 60 (1994).
[27] W. Louisell, *Quantum Statistical Properties of Radiations* (Wiley, New York, 1973).
[28] R. H. Dicke, Phys. Rev. **93**, 99 (1954).
[29] A. Smith and K. Burnett, J. Opt. Soc. Am. B **8**, 1592 (1991).
[30] H. Haken, *Quantum Field Theory of Solids* (North-Holland, Amsterdam, 1976).
[31] V. Chebotayev, B. Dubetsky, A. Kasantsev, and V. Yakovlev, J. Opt. Soc. Am. B **2**, 1791 (1985).
[32] R. Pathria, *Statistical Mechanics* (Pergamon, London, 1972).
[33] S. M. Jensen, IEEE J. Quantum Electron. **QE-18**, 1580 (1982).
[34] Weiping Zhang, D. F. Walls, and B. C. Sanders (unpublished).

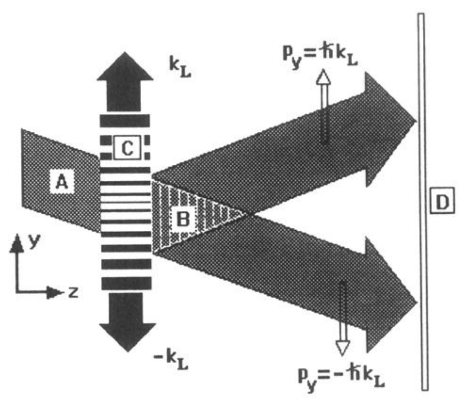

FIG. 1. The schematic diagram for Bragg scattering of an atomic beam by a standing-wave laser beam: *A* denotes the incident atomic beam, *B* the near-field interference region, *C* the standing-wave laser beam, and *D* the detection screen.

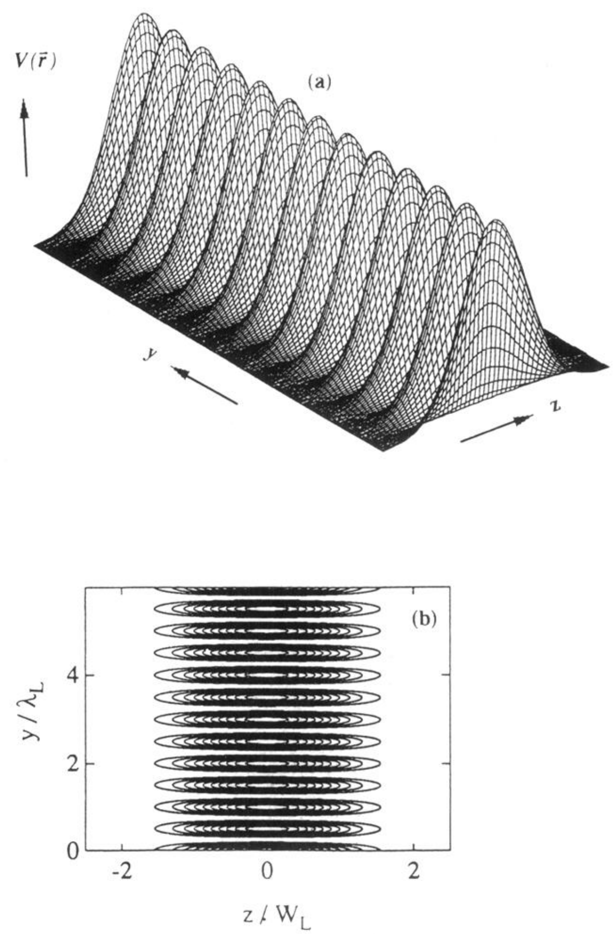

FIG. 2. The dipole potential $V(\mathbf{r})$ for a negligible absorption and dispersion $[(\sqrt{\pi}/2)\sigma w_y \rho_0 = 0.01]$: (a) the spatial structure of the dipole potential, and (b) the contour of the dipole potential in the y-z plane. The detuning chosen are $\Delta = \pm 10\gamma$.

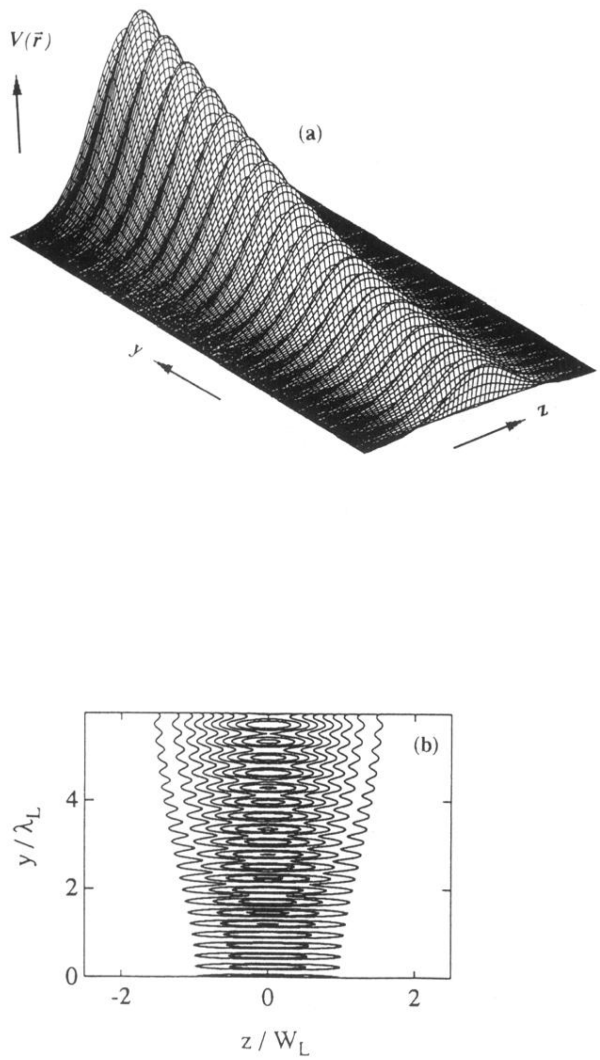

FIG. 3. The dipole potential $V(\mathbf{r})$ for a negative detuning $\Delta = -10\gamma$ and a large absorption and dispersion $[(\sqrt{\pi}/2)\sigma w_y \rho_0 = 3]$: (a) the spatial structure of the dipole potential, and (b) the contour of the dipole potential in the y-z plane.

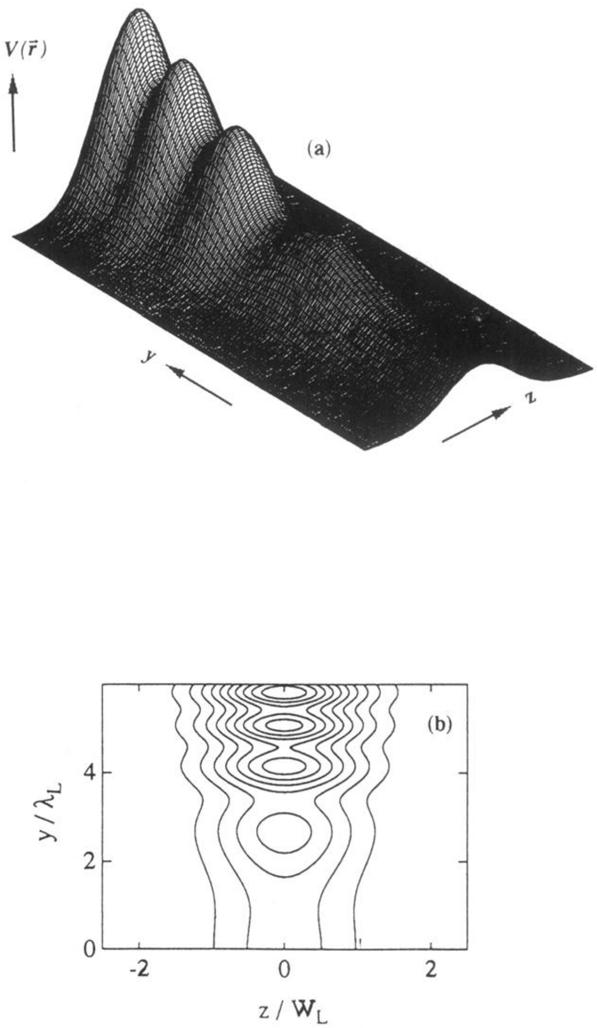

FIG. 4. The dipole potential $V(\mathbf{r})$ for a positive detuning $\Delta=10\gamma$ and a large absorption and dispersion $[(\sqrt{\pi}/2)\sigma w_y \rho_0 = 3]$: (a) the spatial structure of the dipole potential, and (b) the contour of the dipole potential in the y-z plane.

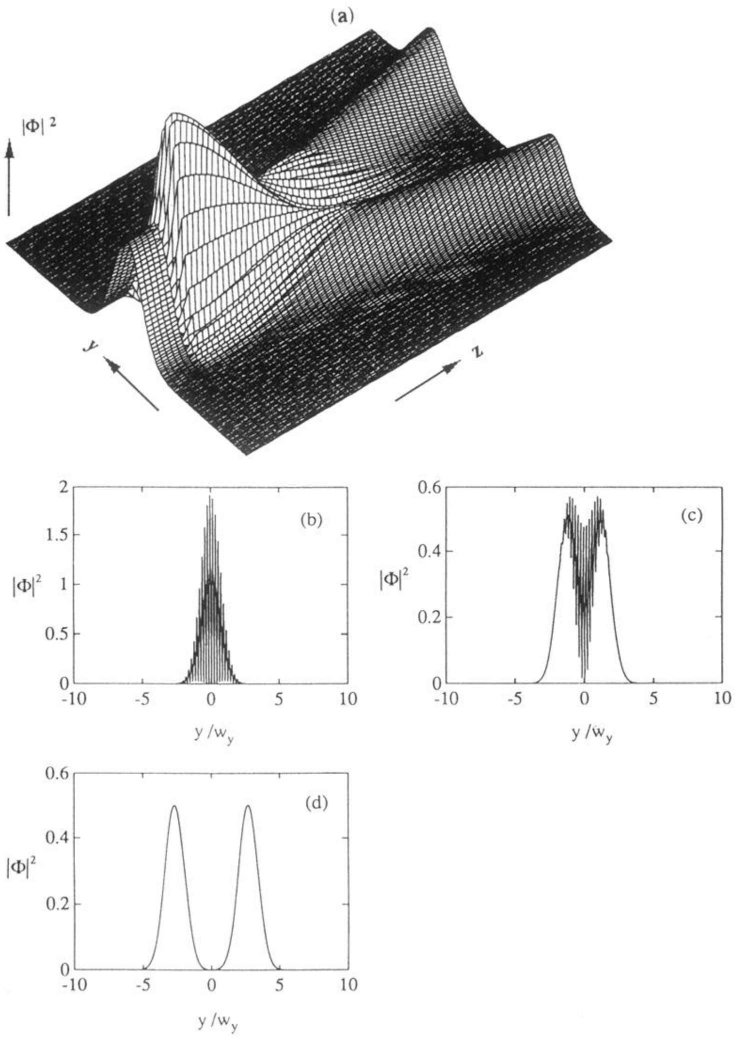

FIG. 5. The density distribution of the atomic beam for linear Bragg scattering. The parameters chosen are $g_0=\pi/4$ and $\beta\rho_0=0.001$. (a) The global density distribution of the atomic beam in propagation, (b) the near-field density distribution with $\tau=2\tau_0$ and the oscillation is due to the near-field interference of the diffracted atomic beams, (c) the near-field density distribution with $\tau=30\tau_0$, and (d) the far-field density distribution with $\tau=60\tau_0$.

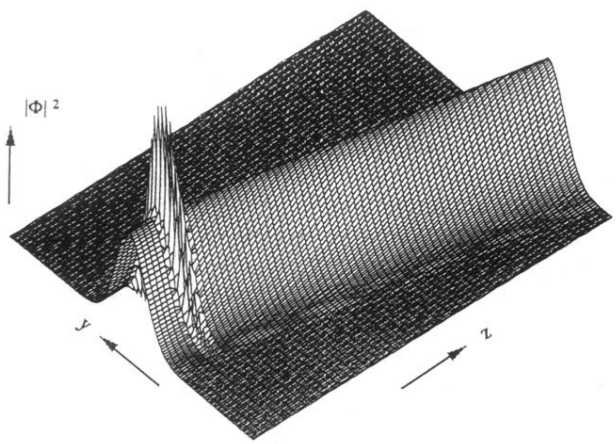

FIG. 6. The global density distribution of the atomic beam for linear Bragg scattering with the parameters chosen as $g_0=\pi$ and $\beta\rho_0=0.001$.

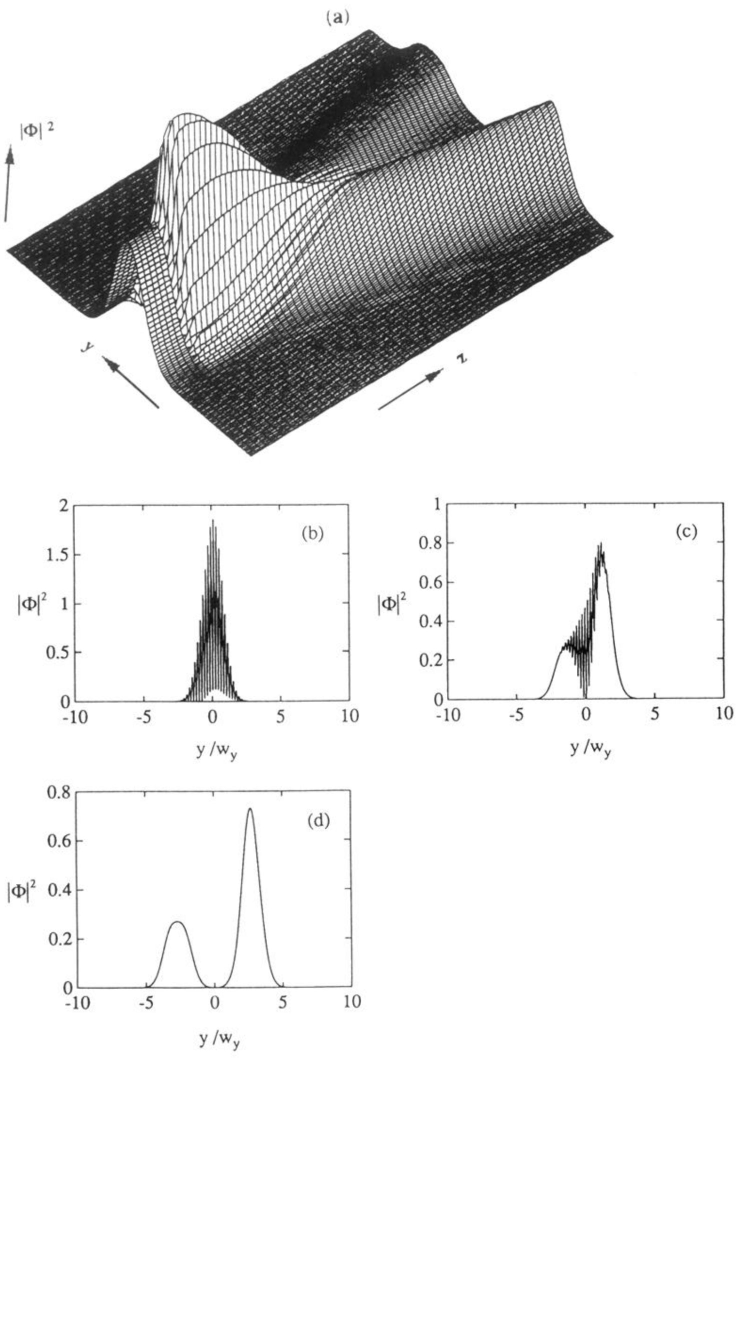

FIG. 7. The density distribution of the atomic beam for nonlinear Bragg scattering. The parameters chosen are $g_0 = \pi/4$ and $\beta\rho_0 = 0.3$. (a) The global density distribution of the atomic beam in propagation, (b) the near-field density distribution with $\tau = 2\tau_0$ and the oscillation is due to the near-field interference of the diffracted atomic beams, (c) the near-field density distribution with $\tau = 30\tau_0$, and (d) the far-field density distribution with $\tau = 60\tau_0$.

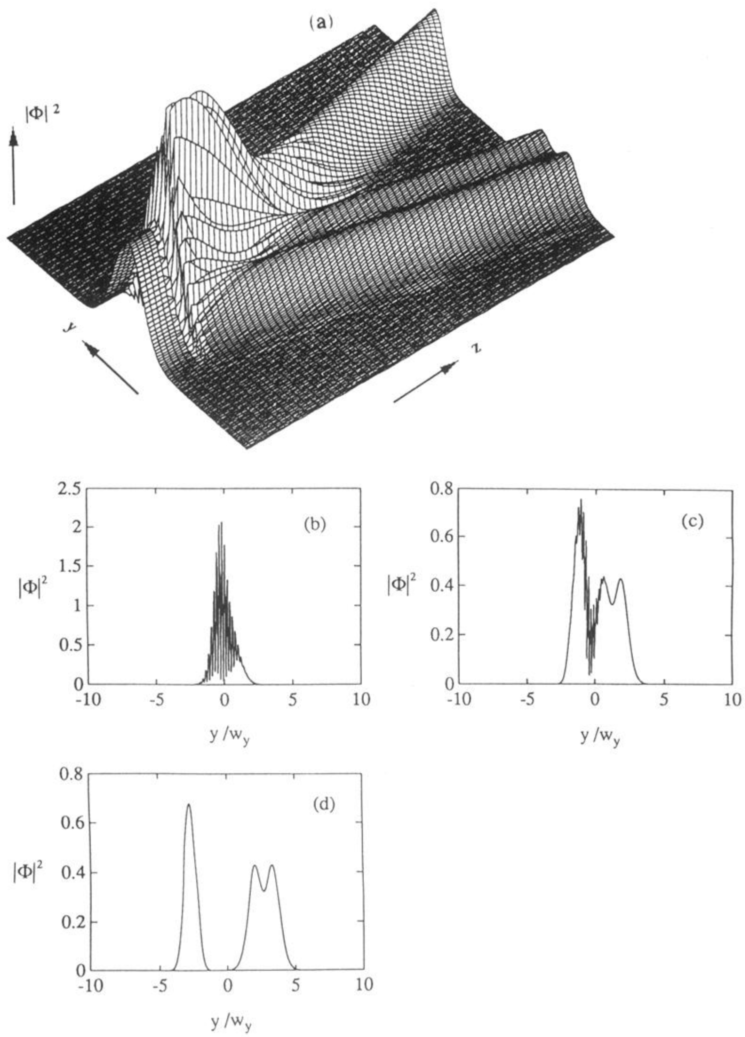

FIG. 8. The density distribution of the atomic beam for nonlinear Bragg scattering. The parameters chosen are $g_0=\pi$ and $\beta\rho_0=0.3$. (a) The global density distribution of the atomic beam in propagation, (b) the near-field density distribution with $\tau=2\tau_0$ and the oscillation is due to the near-field interference of the diffracted atomic beams, (c) the near-field density distribution with $\tau=30\tau_0$, and (d) the far-field density distribution with $\tau=60\tau_0$.

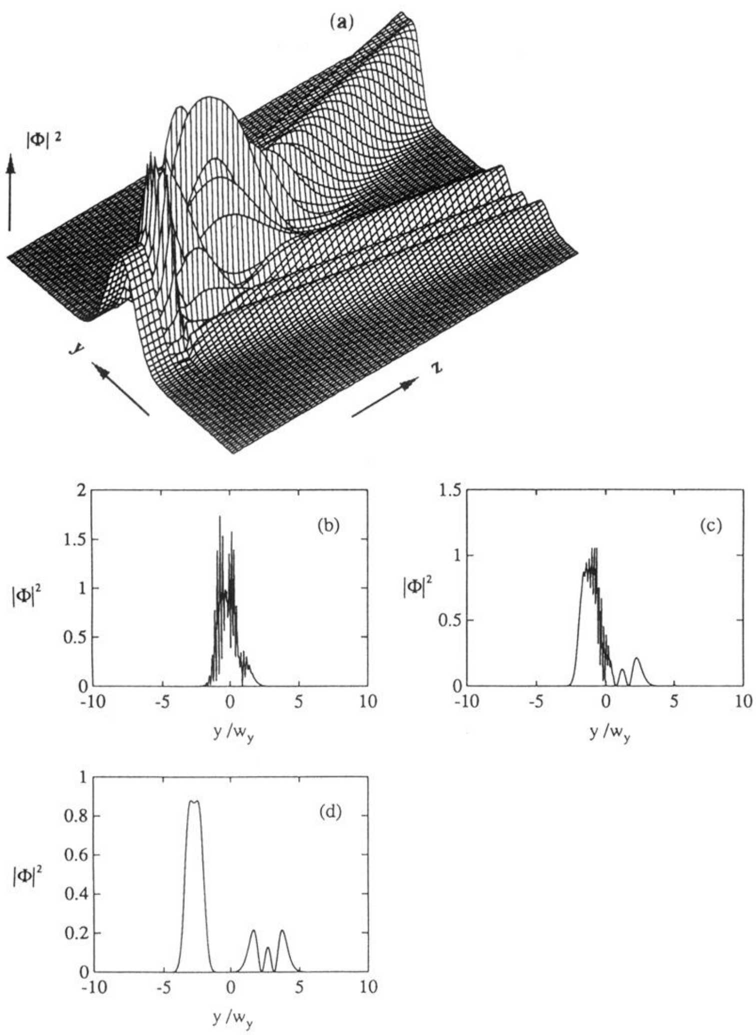

FIG. 9. The density distribution of the atomic beam for nonlinear Bragg scattering. The parameters chosen are $g_0=2\pi$ and $\beta\rho_0=0.3$. (a) The global density distribution of the atomic beam in propagation, (b) the near-field density distribution with $\tau=2\tau_0$ and the oscillation is due to the near-field interference of the diffracted atomic beams, (c) the near-field density distribution with $\tau=30\tau_0$, and (d) the far-field density distribution with $\tau=60\tau_0$.